Computer-Aided Optimization of Particle Accelerators

GSI, Darmstadt, Germany 11-13 March 2015

Non-linear beam dynamics and Frequency Map Analysis

Yannis PAPAPHILIPPOU, CERN

11/03/2015

Contents

- Non-linear beam dynamics and accelerator performance
- Analyzing non-linear motion
  - Accelerator Hamiltonian
  - Accelerator maps
  - Perturbation theory and normal forms
- Chaos detection methods and frequency map analysis
  - Quasi-periodic motion
  - The NAFF algorithm
  - Frequency determination and precision
  - Aspects of frequency maps
- Simulation studies
  - Frequency and diffusion maps for the LHC
  - Beam-beam effect
  - Magnet fringe-fields
  - Working point choice
  - Correction schemes evaluation
- Experiments
  - Experimental frequency maps
  - Beam loss frequency maps
- Summary

Non-linear effects in accelerators

- Non-linear magnets (sextupoles, octupoles)
- Magnet imperfections and misalignments
- Noise (power supply ripple, ground motion)
- Insertion quadrupoles
- Magnets in experimental areas (solenoids, dipoles)
- Injection elements
- Magnet fringe fields
- Insertion devices (wigglers, undulators)
- Beam-beam effect (head on and long range)
- Space-charge effect
- Electron cloud (Ion) effects

- Performance issues
  - Particle losses causing
    - Reduced lifetime
    - Radio-activation (super-conducting magnet quench)
    - Reduced machine availability
  - Emittance blow-up
  - Reduced number of bunches and/or increased crossing angle
  - Reduced intensity
- Cost issues
  - Number of magnet correctors and families (power convertors)
  - Magnetic field and alignment tolerances

Single-particle relativistic Hamiltonian

- Neglecting self fields and radiation, motion can be described by a single-particle Hamiltonian

$$H(\mathbf{x},\mathbf{p},t) = c\sqrt{\left(\mathbf{p} - \frac{e}{c}\mathbf{A}(\mathbf{x},t)\right)^2 + m^2c^2} + e\Phi(\mathbf{x},t)$$

  - $\mathbf{x} = (x, y, z)$ Cartesian positions
  - $\mathbf{p} = (p_x, p_y, p_z)$ conjugate momenta
  - $\mathbf{A} = (A_x, A_y, A_z)$ the magnetic vector potential
  - Φ the electric scalar potential

- The ordinary kinetic momentum vector is written as

$$\mathbf{P} = \gamma m\mathbf{v} = \mathbf{p} - \frac{e}{c}\mathbf{A}$$

with $\mathbf{v}$ the velocity vector and $\gamma = (1 - v^2/c^2)^{-1/2}$ the relativistic factor

Accelerator Hamiltonian

- Introduce **approximations**
  - Neglect electric potential (decouple synchrotron motion from transverse)
  - Consider only static transverse magnetic fields, so vector potential has only one longitudinal component

$$A_s(x,y,s) = \left(1 + \frac{x}{\rho(s)}\right) B_0 \Re e \sum_{n=0}^{\infty} \frac{b'_n(s) - i a'_n(s)}{n+1} (x+iy)^{n+1}$$

  - Consider total momentum much higher than transverse (true for high-energy) and expand the square root to 1st order
  - Impose that radius of curvature $\rho(s)$ is much larger than transverse position (large ring approximation)
- Apply **canonical transformations**, by first setting the independent variable as the path length s and move the periodic orbit to the origin

$$\mathcal{H} = \frac{p_x^2 + p_y^2}{2(1+\delta)} - \frac{x(1+\delta)}{\rho(s)} - e\hat{A}_s \quad \text{with} \quad \delta \equiv \frac{P_t - P_0}{P_0}$$

Classical perturbation theory

- It is convenient to write the Hamiltonian like an integrable part plus a perturbation

$$\mathcal{H}(x, y, p_x, p_y, s) = \mathcal{H}_0(x, y, p_x, p_y, s) + \sum_{k_x, k_y} h_{k_x, k_y}(s) x^{k_x} y^{k_y}$$

where the polynomial coefficients are periodic $h_{k_x,k_y}(s) = h_{k_x,k_y}(s + C)$

- The integrable Hamiltonian is derived by considering only dipole (uniform) fields normal quadrupole (linear) magnetic fields, with normalized gradient $K(s)$

$$\mathcal{H}_0 = \frac{p_x^2 + p_y^2}{2(1+\delta)} - \frac{x\delta}{\rho(s)} + \frac{x^2}{2\rho(s)^2} + \frac{K(s)}{2}(x^2 - y^2)$$

- Classical perturbation theory already applied in the early days of the first synchrotrons for analyzing non-linear part (resonance driving terms)

J. Moser, CERN Symp, HEACC, 1956;
R. Hagedorn, CERN Yellow Report 57-1, 1957;
A. Shoch, CERN Yellow Report, 57-21, 1958

Accelerator Maps

A.J. Dragt and J.M. Finn, J. Math. Phys. 17, 2215, 1976;
A.J. Dragt, IEEE Trans. Nucl. Sc., NS-26, No. 3, 3601,1979

- Lie formalism was introduced for representing symplectic accelerator maps
- For a Hamiltonian system $H(\mathbf{z},t)$ there is a formal solution of the equations of motion $\frac{d\mathbf{z}}{dt} = [H,\mathbf{z}] =: H : \mathbf{z}$ written as $\mathbf{z}(t) = \sum_{k=0}^{\infty} \frac{t^k :H:^k}{k!}\mathbf{z}_0 = e^{t:H:}\mathbf{z}_0$, with $\mathcal{M} = e^{:H:}$ a symplectic map
- The 1-turn accelerator map is represented by the composition of the maps of each element $\mathcal{M} = e^{:f_2:}\ e^{:f_3:}\ e^{:f_4:}\ \ldots$
- Differential algebra tools can be used for computing efficiently the map
- Normal form approaches can be applied to the numerically constructed map

E. Forest, M. Berz, and J. Irwin, PA, 24, 91, 1989;
M. Berz, PA, 24, 109, 1989;
A. Bazzani, G. Servizi, E. Todesco, and G. Turchetti, CERN Yellow Report, 94-02, 1994.

Normal form analysis of LHC models

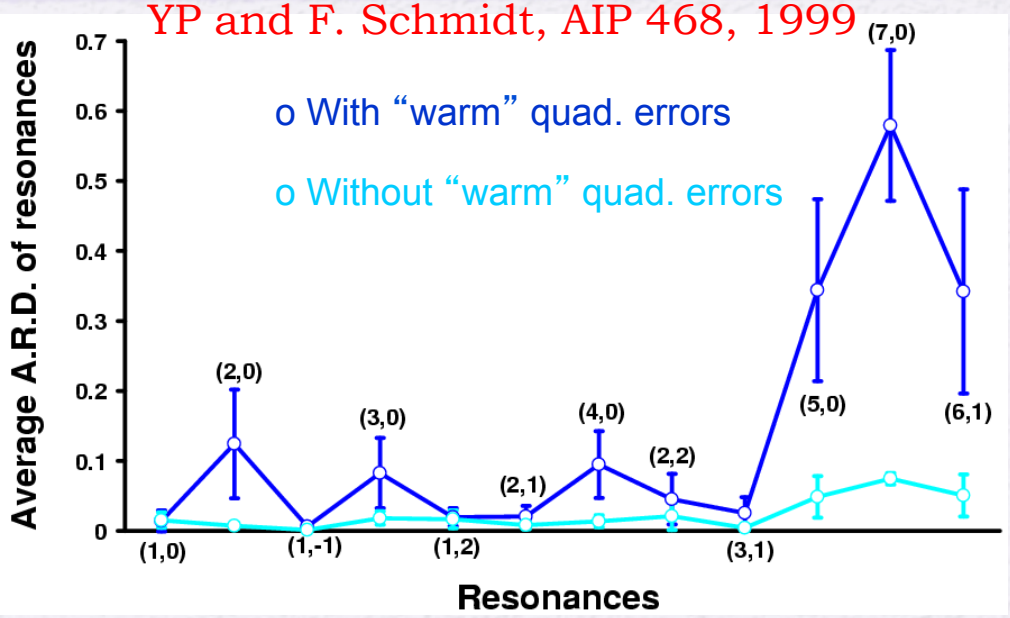

Phase	Type	DA (σ)	LHC Version		
			4	5	
				Nominal	Target
15°	Warm Quads switched ON	Average	10.0	9.1	10.4
		Minimum	8.5	7.4	8.6
	Warm Quads switched OFF	Average	10.7	11.5	12.4
		Minimum	9.6	10.3	11.3
45°	Warm Quads switched ON	Average	11.1	11.3	12.8
		Minimum	9.5	9.2	11.4
	Warm Quads switched OFF	Average	11.4	12.4	13.8
		Minimum	10.1	10.7	12.3

- In the LHC at injection (450 GeV), beam stability is necessary over a very large number of turns (10^7)
- Stability is reduced from random multi-pole imperfections mainly in the super-conducting magnets
- Area of stability (Dynamic aperture - DA) computed with particle tracking for a large number of random magnet error distributions
- A numerical tool based on normal form analysis (GRR) permitted the identification of the reason for the DA reduction between two versions of the LHC optics (errors in the "warm" quadrupoles)

Chaos detection methods in particle accelerators

- Computing/measuring dynamic aperture (DA) or particle survival

  A. Chao et al., PRL 61, 24, 2752, 1988;
  F. Willeke, PAC95, 24, 109, 1989.

- Computation of Lyapunov exponents

  F. Schmidt, F. Willeke and F. Zimmermann, PA, 35, 249, 1991;
  M. Giovannozi, W. Scandale and E. Todesco, PA 56, 195, 1997

- Variance of unperturbed action (a la Chirikov)

  B. Chirikov, J. Ford and F. Vivaldi, AIP CP-57, 323, 1979
  J. Tennyson, SSC-155, 1988;
  J. Irwin, SSC-233, 1989

- Fokker-Planck diffusion coefficient in actions

  T. Sen and J.A. Elisson, PRL 77, 1051, 1996

- **Frequency map analysis**

Frequency map analysis

- Frequency Map Analysis (FMA) is a numerical method which springs from the studies of J. Laskar (Paris Observatory) putting in evidence the chaotic motion in the Solar Systems
- FMA was successively applied to several dynamical systems
  - Celestial mechanics J.Laskar and P.Robutel, Nature 361, 608, 1993
  - 4D maps J.Laskar, Physica D 67, 257–281, 1993
  - Galactic Dynamics Y.P. and J.Laskar, A&A, 307, 427, 1996
    Y.P. and J.Laskar, A&A, 329, 451, 1998
  - Accelerator beam dynamics: lepton and hadron rings

H.S.Dumas and J.Laskar, PRL 70, 2975, 1993
J.Laskar and D.Robin, Part.Accel. 54, 183, 1996
Y.P, PAC99, 1554, 1999
L.Nadolski and J.Laskar, PRSTAB 6, 114801, 2003
Y.P., Chaos, 24, 024412, 2014

Motion on torus

- Consider an integrable Hamiltonian system of the usual form

$$H(\boldsymbol{J}, \boldsymbol{\varphi}, \theta) = H_0(\mathbf{J})$$

- Hamilton's equations give

$$\dot{\phi}_j = \frac{\partial H_0(\mathbf{J})}{\partial J_j} = \omega_j(\mathbf{J}) \Rightarrow \phi_j = \omega_j(\mathbf{J})t + \phi_{j0}$$

$$\dot{J}_j = -\frac{\partial H_0(\mathbf{J})}{\partial \phi_j} = 0 \Rightarrow J_j = \text{const.}$$

- The actions define the surface of an invariant torus
- In complex coordinates the motion is described by

$$\zeta_j(t) = J_j(0)e^{i\omega_j t} = z_{j0}e^{i\omega_j t}$$

- For a **non-degenerate** system $\det\left|\frac{\partial \omega(J)}{\partial J}\right| = \det\left|\frac{\partial^2 H_0(J)}{\partial J^2}\right| \neq 0$ there is a one-to-one correspondence between the actions and the frequency, a frequency map can be defined parameterizing the tori in the frequency space

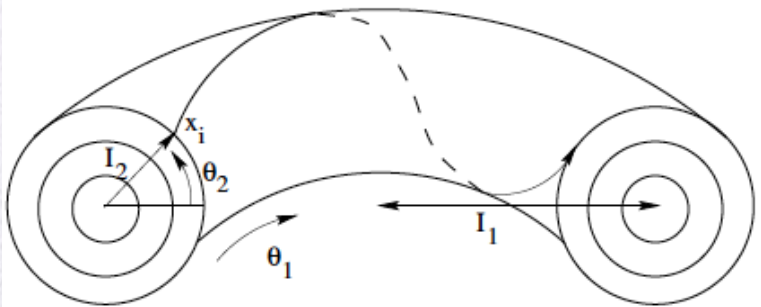

Quasi-periodic motion

- If a transformation is made to some new variables

$$\zeta_j = I_j e^{i\theta_j t} = z_j + \epsilon G_j(\mathbf{z}) = z_j + \epsilon \sum_{\mathbf{m}} c_{\mathbf{m}} z_1^{m_1} z_2^{m_2} \dots z_n^{m_n}$$

- The system is still integrable but the tori are distorted
- The motion is then described by

$$\zeta_j(t) = z_{j0} e^{i\omega_j t} + \sum_{\mathbf{m}} a_{\mathbf{m}} e^{i\,(\mathbf{m}\cdot\omega)\,t}$$

  i.e. a quasi-periodic function of time, with

$$a_{\mathbf{m}} = \epsilon\, c_{\mathbf{m}} z_{10}^{m_1} z_{20}^{m_2} \dots z_{n0}^{m_n} \text{ and } \mathbf{m}\cdot\omega = m_1\omega_1 + m_2\omega_2 + \dots + m_n\omega_n$$

- For a non-integrable Hamiltonian, $H(\mathbf{I},\theta) = H_0(\mathbf{I}) + \epsilon H'(\mathbf{I},\theta)$ it and especially if the perturbation is small, most tori persist (**KAM** theory)
- In that case, the motion is still quasi-periodic and a frequency map can be built
- The regularity (or not) of the map reveals stable (or chaotic) motion

Building the frequency map

- When a quasi-periodic function $f(t) = q(t) + ip(t)$ in the complex domain is given numerically, it is possible to recover a quasi-periodic approximation

$$f'(t) = \sum_{k=1}^{N} a'_k e^{i\omega'_k t}$$

in a very precise way over a finite time span $[-T, T]$ several orders of magnitude more precisely than simple Fourier techniques

- This approximation is provided by the Numerical Analysis of Fundamental Frequencies – **NAFF** algorithm
- The frequencies ω'_k and complex amplitudes a'_k are computed through an iterative scheme.

Diffusion in frequency space

- For a 2 degrees of freedom Hamiltonian system, the frequency space is a line, the tori are dots on this lines, and the chaotic zones are confined by the existing KAM tori

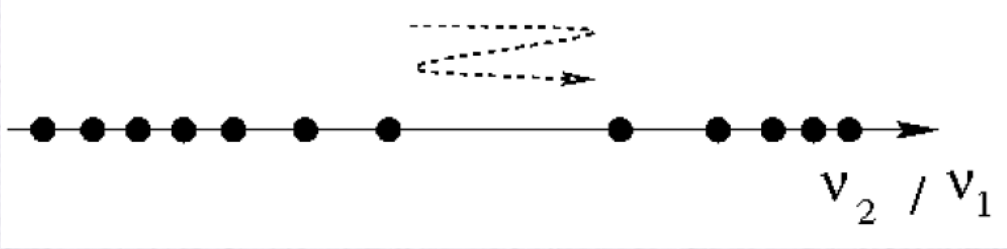

- For a system with 3 or more degrees of freedom, KAM tori are still represented by dots but do not prevent chaotic trajectories to diffuse
- This diffusion is supposed to be extremely small in their vicinity, as tori act as effective barriers (Nechoroshev theory)

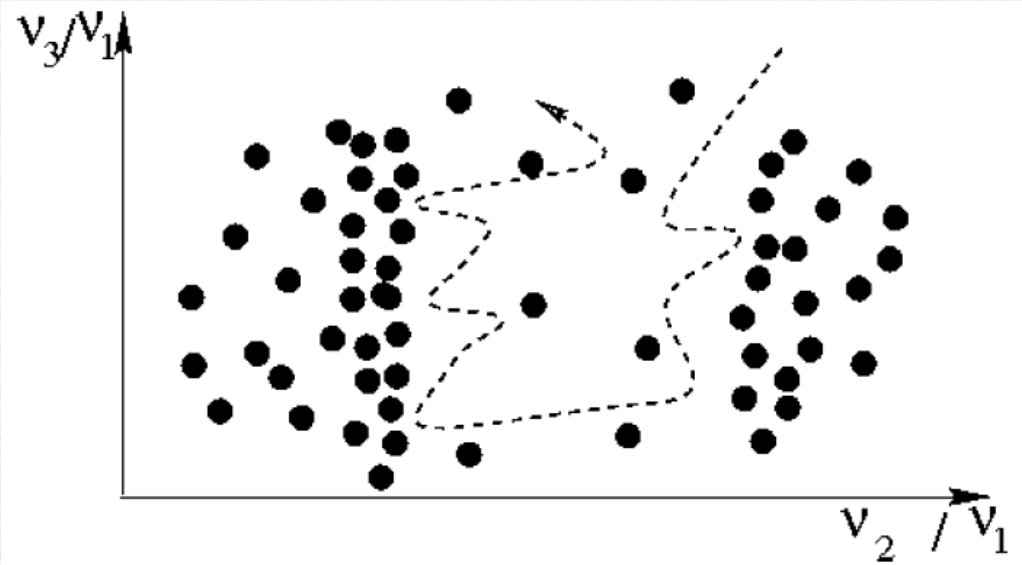

Aspects of the frequency map

- In the vicinity of a resonance the system behaves like a pendulum
- Passing through the elliptic point for a fixed angle, a fixed frequency (or rotation number) is observed
- Passing through the hyperbolic point, a frequency jump is observed

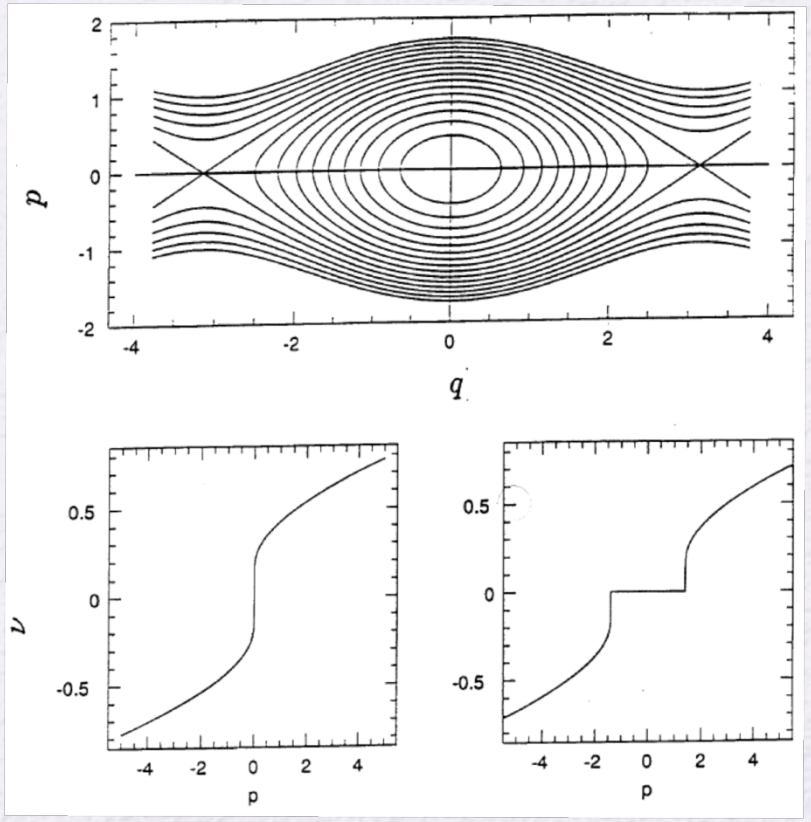

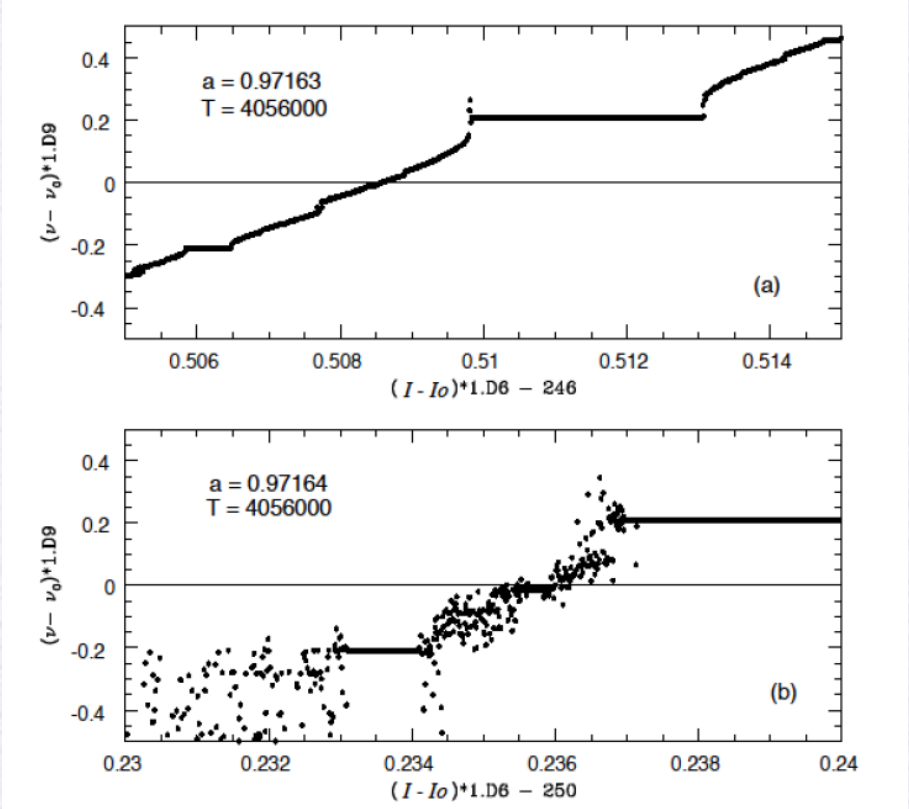

Building the Frequency Map in practice

- Choose initial condition (x_i, y_i) with $(p_{xi}, p_{yi}) = (0, 0)$
- Numerically integrate trajectories through the accelerator for sufficient number of turns (around 1000)
- Compute through NAFF, the associated frequencies of motion
- Plot them in the frequency diagram (tune footprint)

$$\begin{array}{rccc} \mathcal{F}_\tau : & \mathbb{R}^2 & \longrightarrow & \mathbb{R}^2 \\ & (I_x, I_y)|_{p_x, p_y = 0}, & \longrightarrow & (\nu_x, \nu_y) \end{array}$$

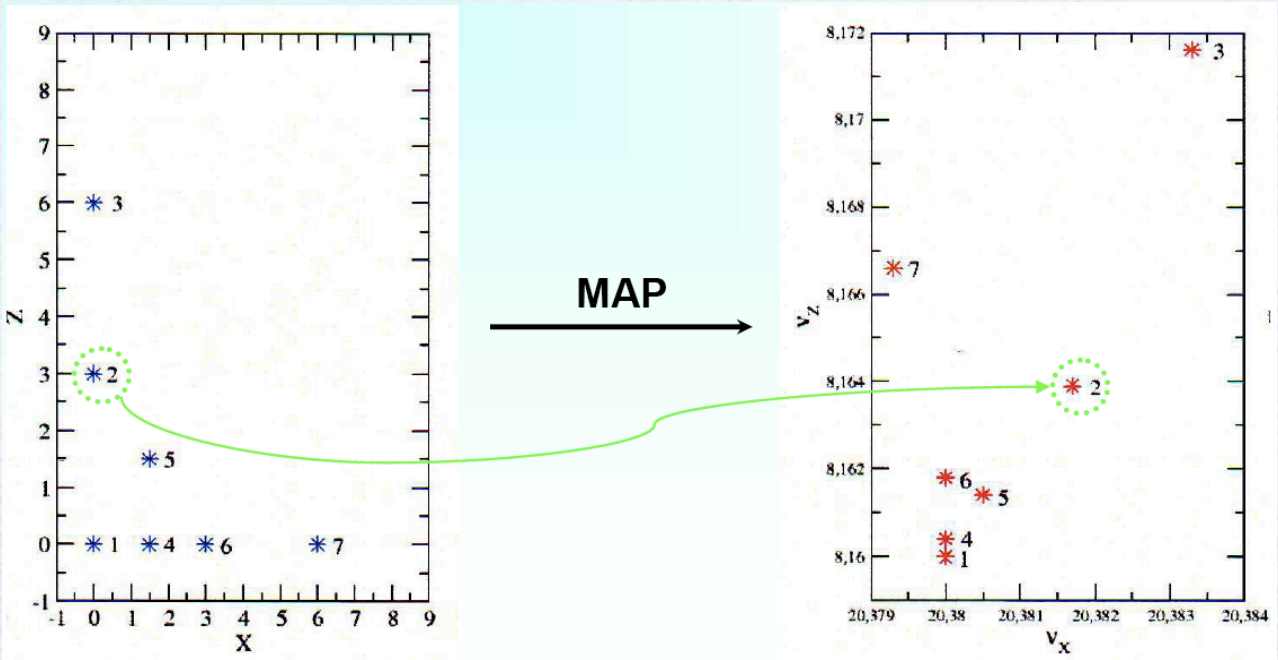

Frequency maps for the LHC

Y. P., PAC99, 1554, 1999

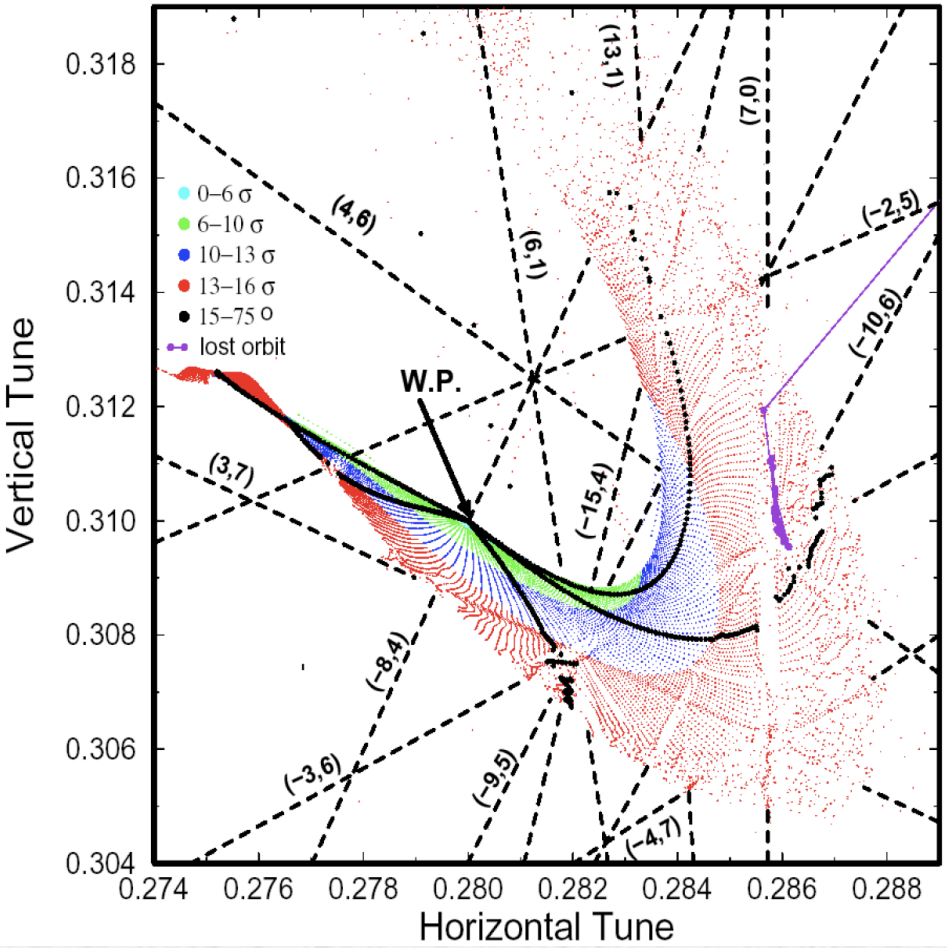

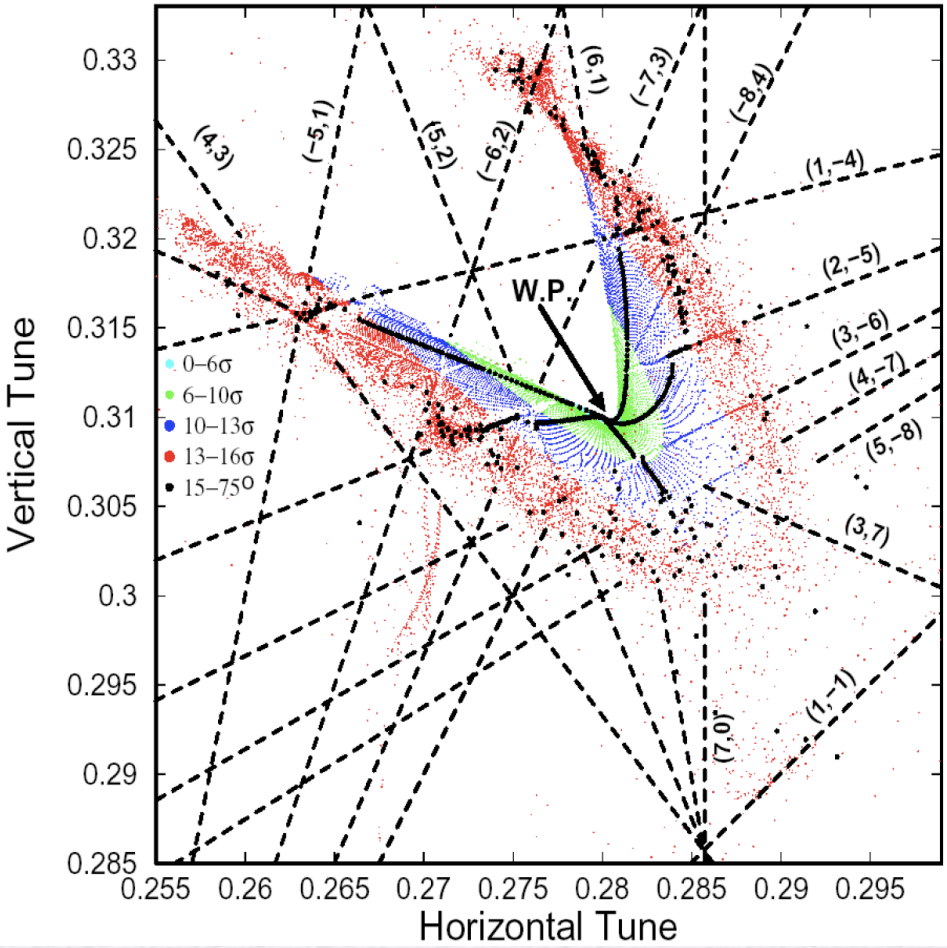

Frequency maps for the target error table (left) and an increased random skew octupole error in the super-conducting dipoles (right)

Diffusion Maps

J. Laskar, PhysicaD, 1993

- Calculate frequencies for two equal and successive time spans and compute frequency diffusion vector:

$$\boldsymbol{D}|_{t=\tau} = \boldsymbol{\nu}|_{t\in(0,\tau/2]} - \boldsymbol{\nu}|_{t\in(\tau/2,\tau]}$$

- Plot the initial condition space color-coded with the norm of the diffusion vector
- Compute a diffusion quality factor by averaging all diffusion coefficients normalized with the initial conditions radius

$$D_{QF} = \left\langle \frac{|\boldsymbol{D}|}{(I_{x0}^2 + I_{y0}^2)^{1/2}} \right\rangle_R$$

Diffusion maps for the LHC

Y. P., PAC99, 1554, 1999

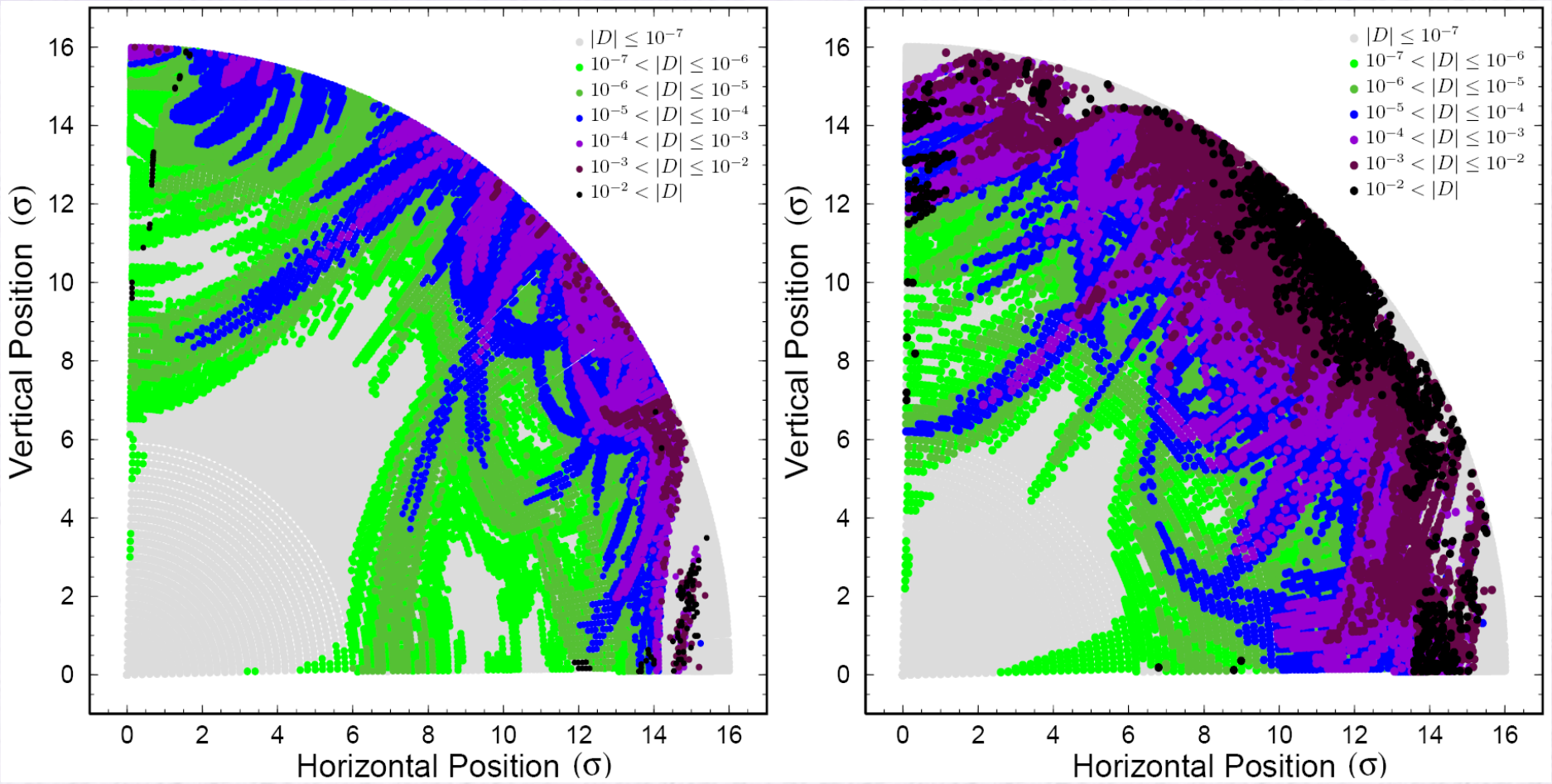

Diffusion maps for the target error table (left) and an increased random skew octupole error in the super-conducting dipoles (right)

Correction schemes efficiency

Y. P., EPAC2000

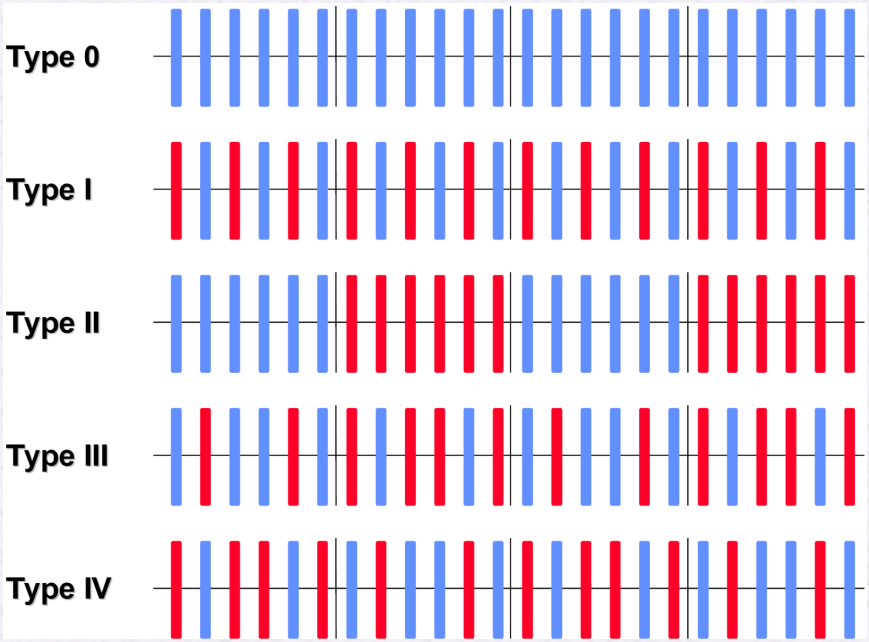

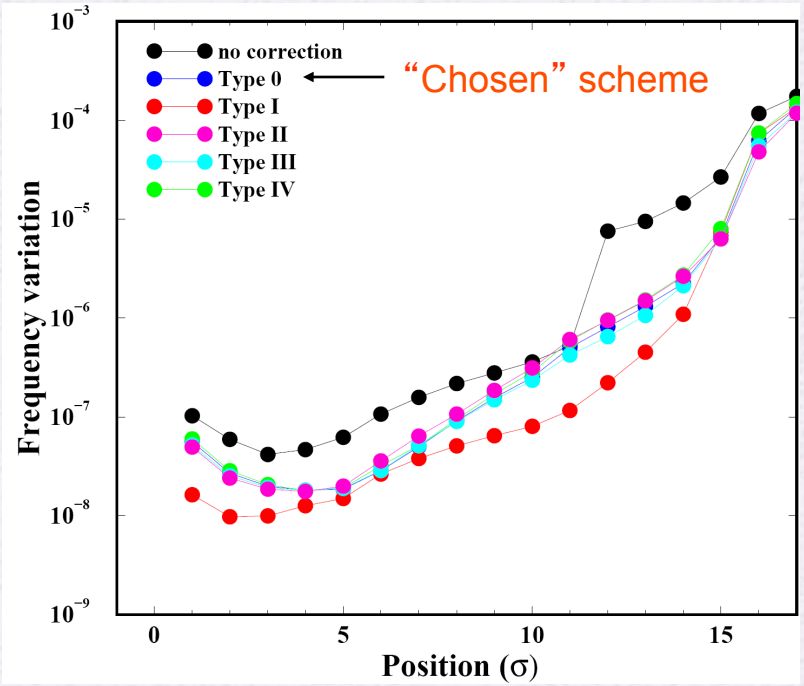

- Comparison of correction schemes for b_4 and b_5 errors in the LHC dipoles
- Frequency maps, resonance analysis, tune diffusion estimates, survival plots and short term tracking, proved that only half of the correctors are needed

Beam-Beam interaction

Variable	Symbol	Value
Beam energy	E	7 TeV
Particle species	$\cdots$	protons
Full crossing angle	θ_c	300 μrad
rms beam divergence	σ'_x	31.7 μrad
rms beam size	σ_x	15.9 μm
Normalized transv. rms emittance	$\gamma\varepsilon$	3.75 μm
IP beta function	β^*	0.5 m
Bunch charge	N_b	$(1 \times 10^{11} - 2 \times 10^{12})$
Betatron tune	Q_0	0.31

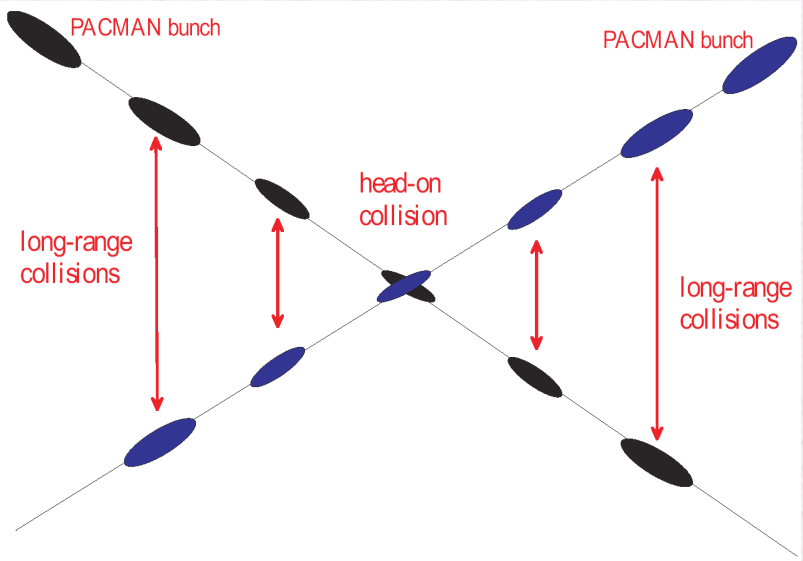

Long range beam-beam interaction represented by a 4D kick-map

$$\Delta x = -\, n_{par}\, \frac{2 r_p N_b}{\gamma} \left[\frac{x' + \theta_c}{\theta_t^2} \left(1 - e^{-\frac{\theta_t^2}{2\theta_{x,y}^2}} \right) - \frac{1}{\theta_c} \left(1 - e^{-\frac{\theta_c^2}{2\theta_{x,y}^2}} \right) \right]$$

$$\Delta y = -\, n_{par}\, \frac{2 r_p N_b}{\gamma}\, \frac{y'}{\theta_t^2} \left(1 - e^{-\frac{\theta_t^2}{2\theta_{x,y}^2}} \right)$$

with $$\theta_t \equiv \left((x' + \theta_c)^2 + y'^2 \right)^{1/2}$$

Head-on vs Long range interaction

Y.P. and F.Zimmermann, PRSTAB 1999, 2002

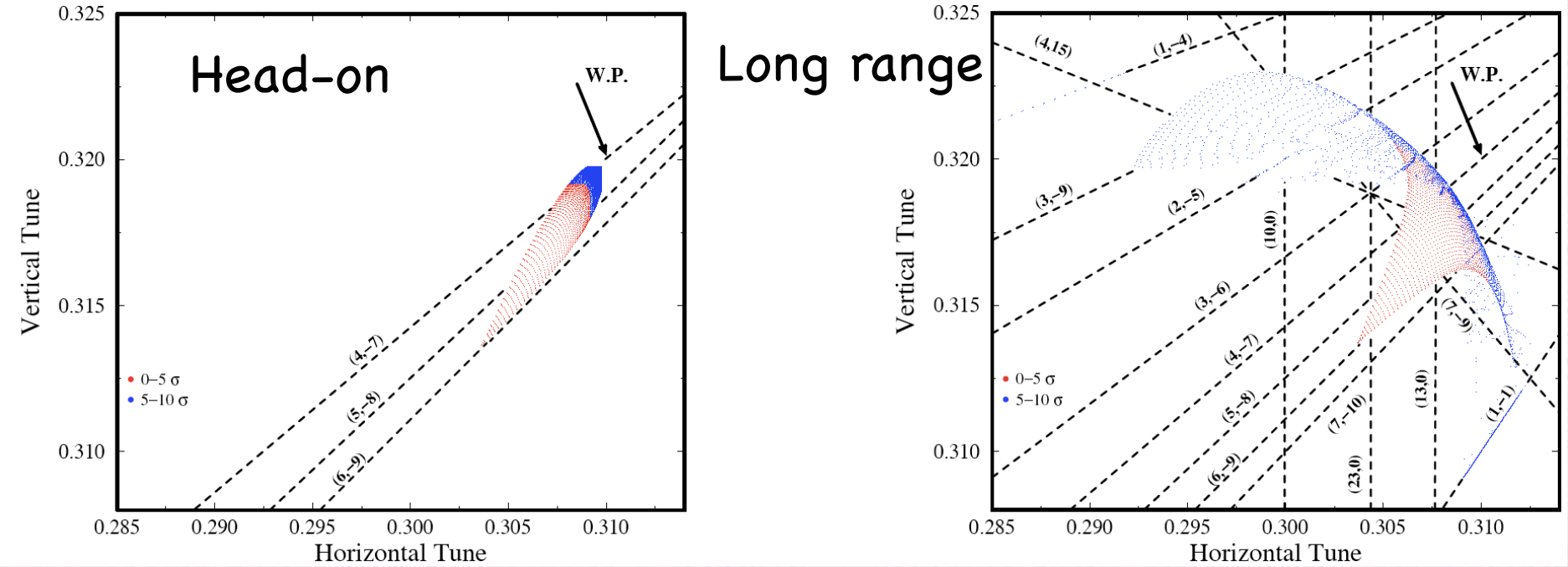

- Proved dominant effect of long range beam-beam effect
- Dynamic Aperture (around 6 σ) located at the folding of the map (indefinite torsion)
- Dynamics dominated by the 1/r part of the force, reproduced by electrical wire, which was proposed for correcting the effect

Action variance vs. frequency diffusion coefficient

Y.P. and F.Zimmermann, PRSTAB 1999, 2002

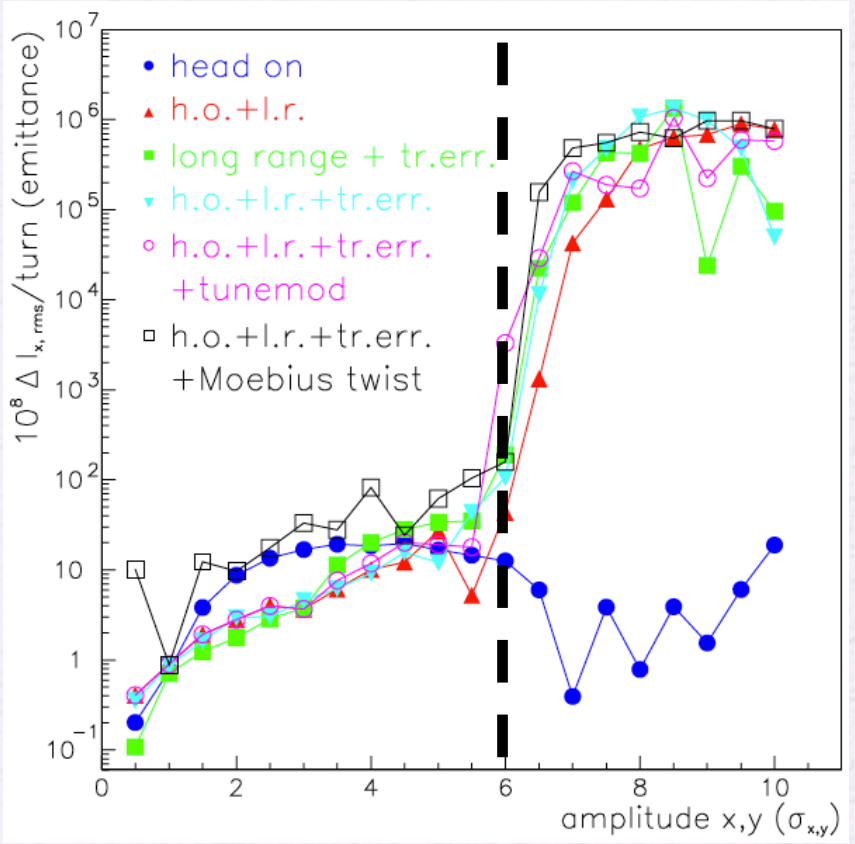

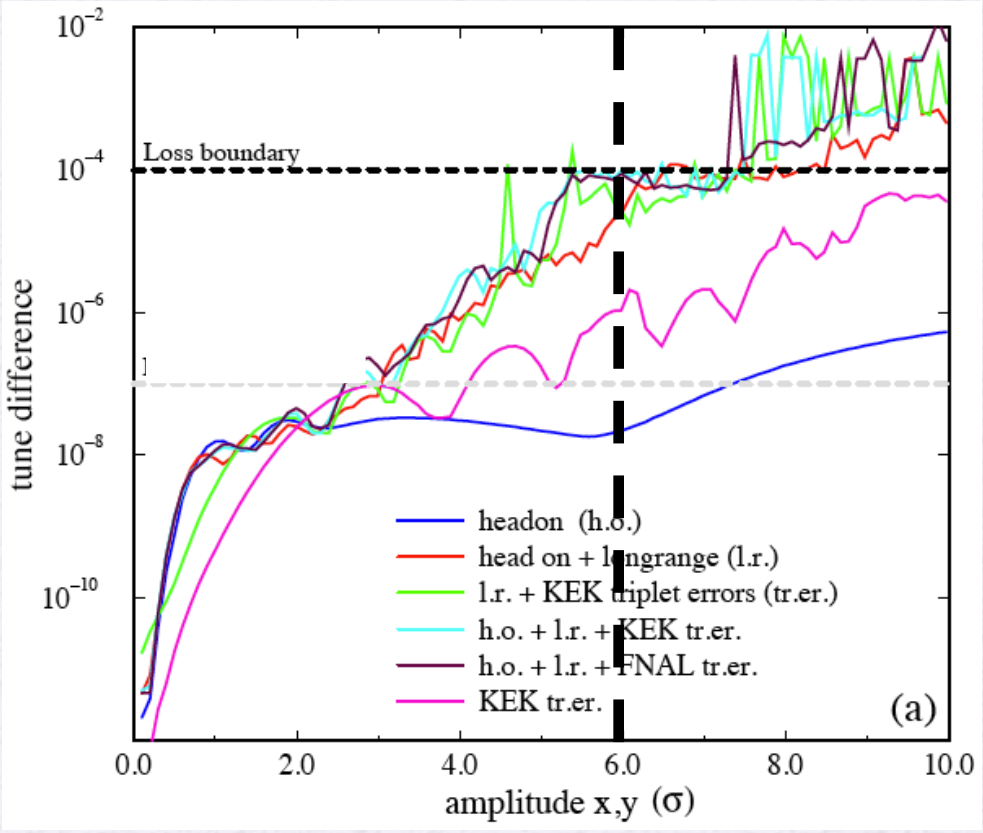

- Very good agreement of diffusive aperture boundary (action variance) with frequency variation (loss boundary corresponding to around 1 frequency unit change in 10^7 turns)

Magnet fringe fields

Y. P. and D.T. Abell, EPAC2000

- From the hard-edge Hamiltonian

$$H_f = \frac{\pm Q}{12B\rho(1+\frac{\delta p}{p})}(y^3 p_y - x^3 p_x + 3x^2 y p_y - 3y^2 x p_x),$$

the first order shift of the frequencies with amplitude can be computed analytically

$$\begin{pmatrix}\delta\nu_x\\ \delta\nu_y\end{pmatrix} = \begin{pmatrix}a_{hh} & a_{hv}\\ a_{hv} & a_{vv}\end{pmatrix}\begin{pmatrix}2J_x\\ 2J_y\end{pmatrix},$$

with the "anharmonicity" coefficients (torsion)

$$a_{hh} = \frac{-1}{16\pi B\rho}\sum_i \pm Q_i \beta_{xi}\alpha_{xi}$$
$$a_{hv} = \frac{1}{16\pi B\rho}\sum_i \pm Q_i (\beta_{xi}\alpha_{yi} - \beta_{yi}\alpha_{xi})$$
$$a_{vv} = \frac{1}{16\pi B\rho}\sum_i \pm Q_i \beta_{yi}\alpha_{yi}$$

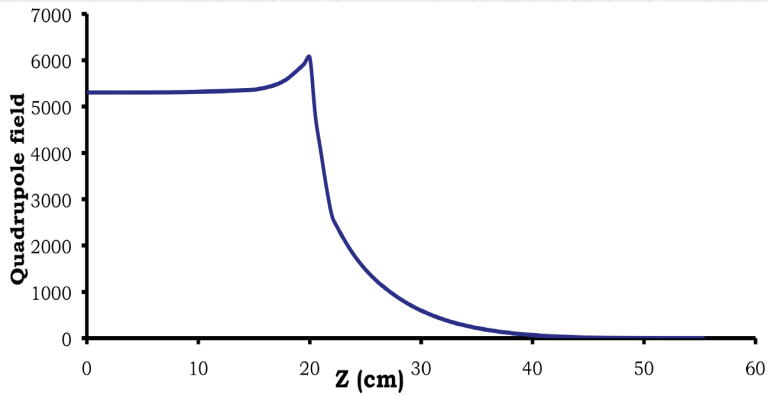

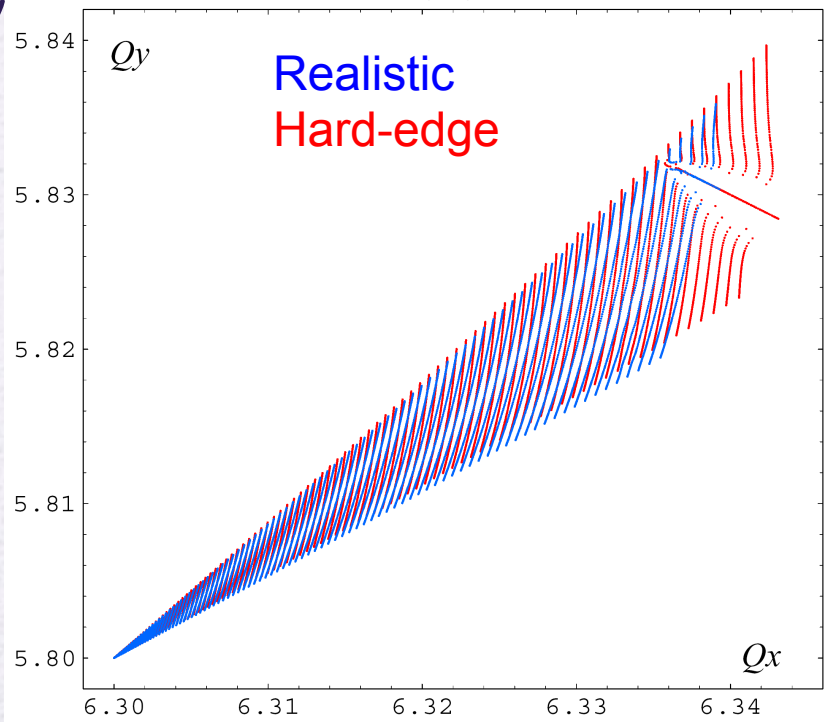

Off-momentum frequency maps

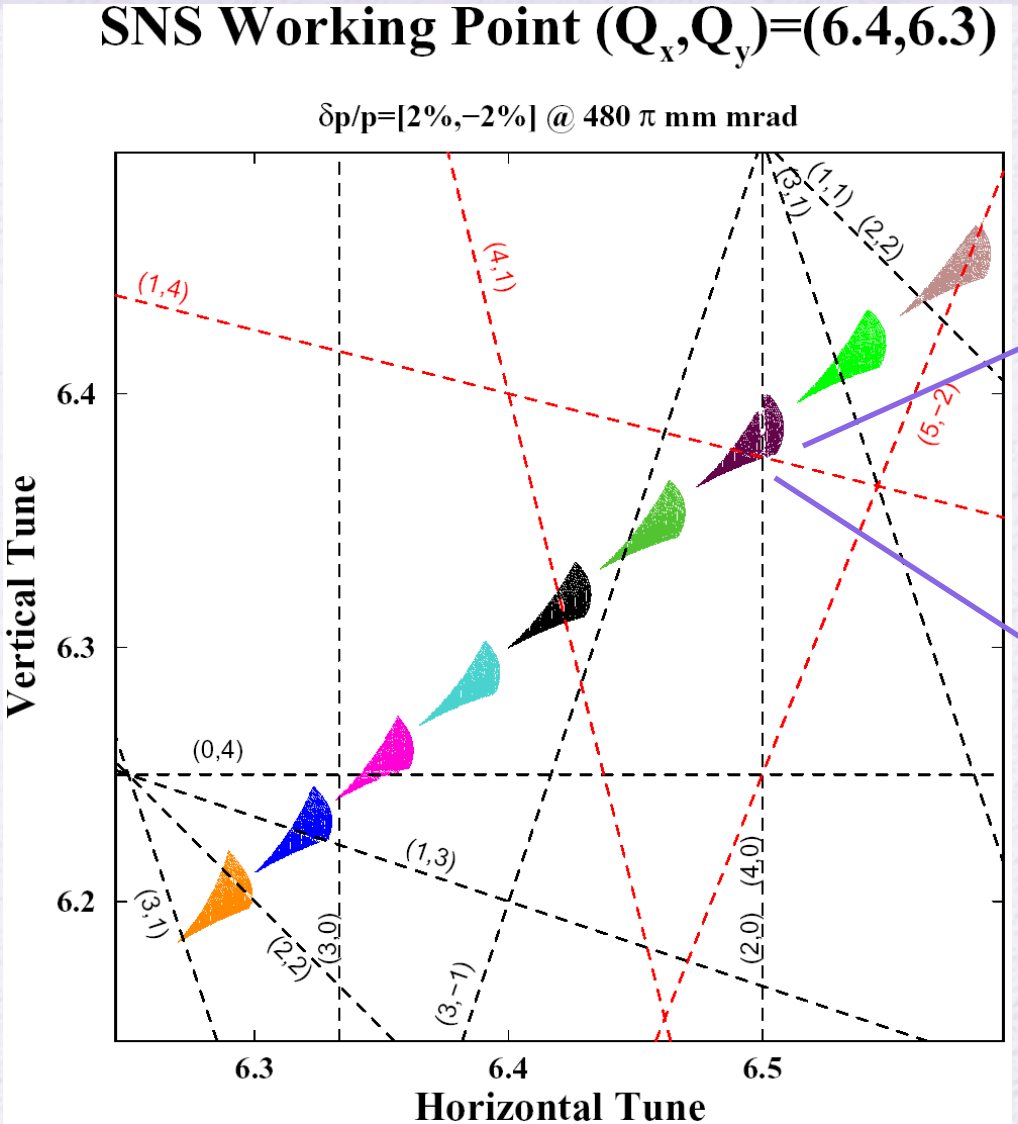

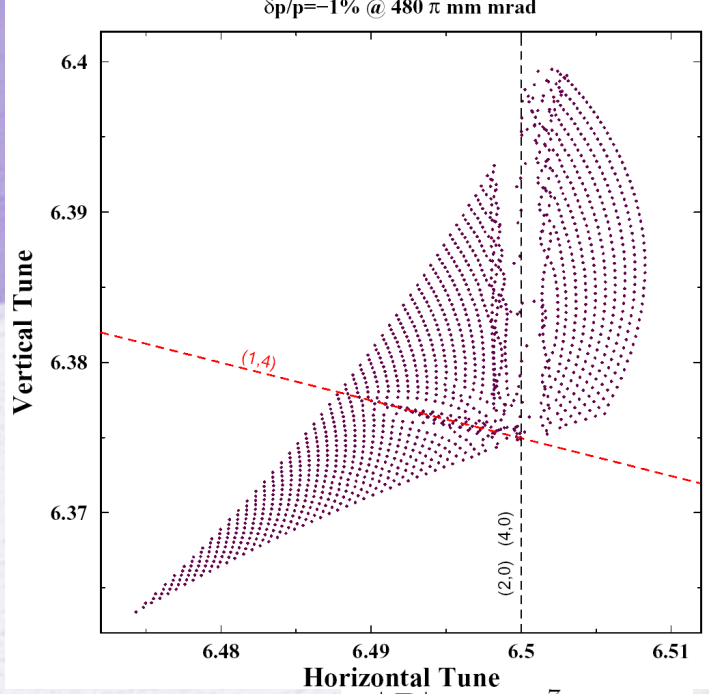

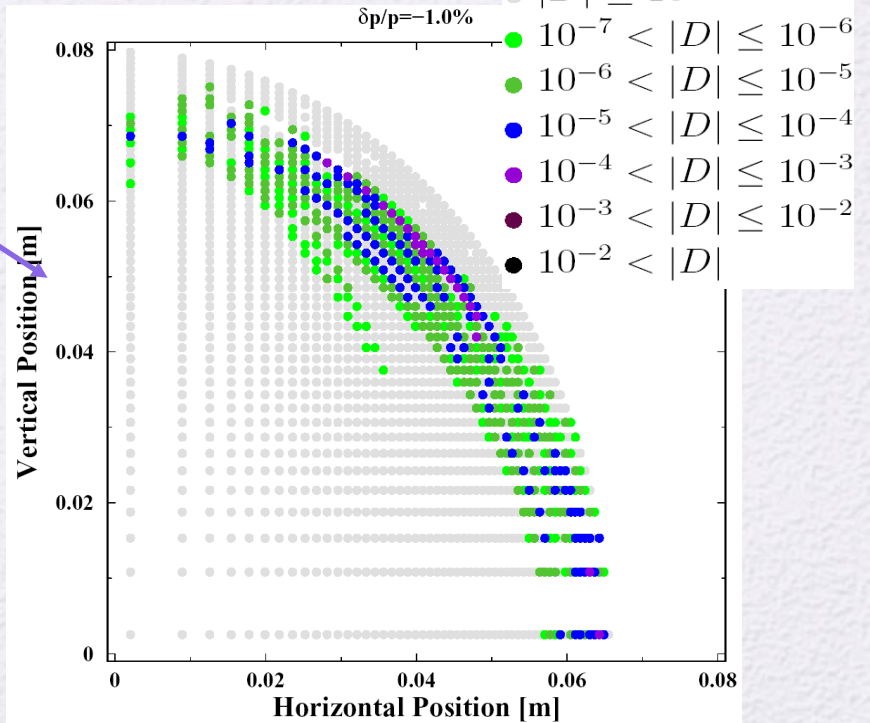

Choice of the SNS ring working point

Tune Diffusion quality factor

$$D_{QF} = \left\langle \frac{|\boldsymbol{D}|}{(I_{x0}^2 + I_{y0}^2)^{1/2}} \right\rangle_R$$

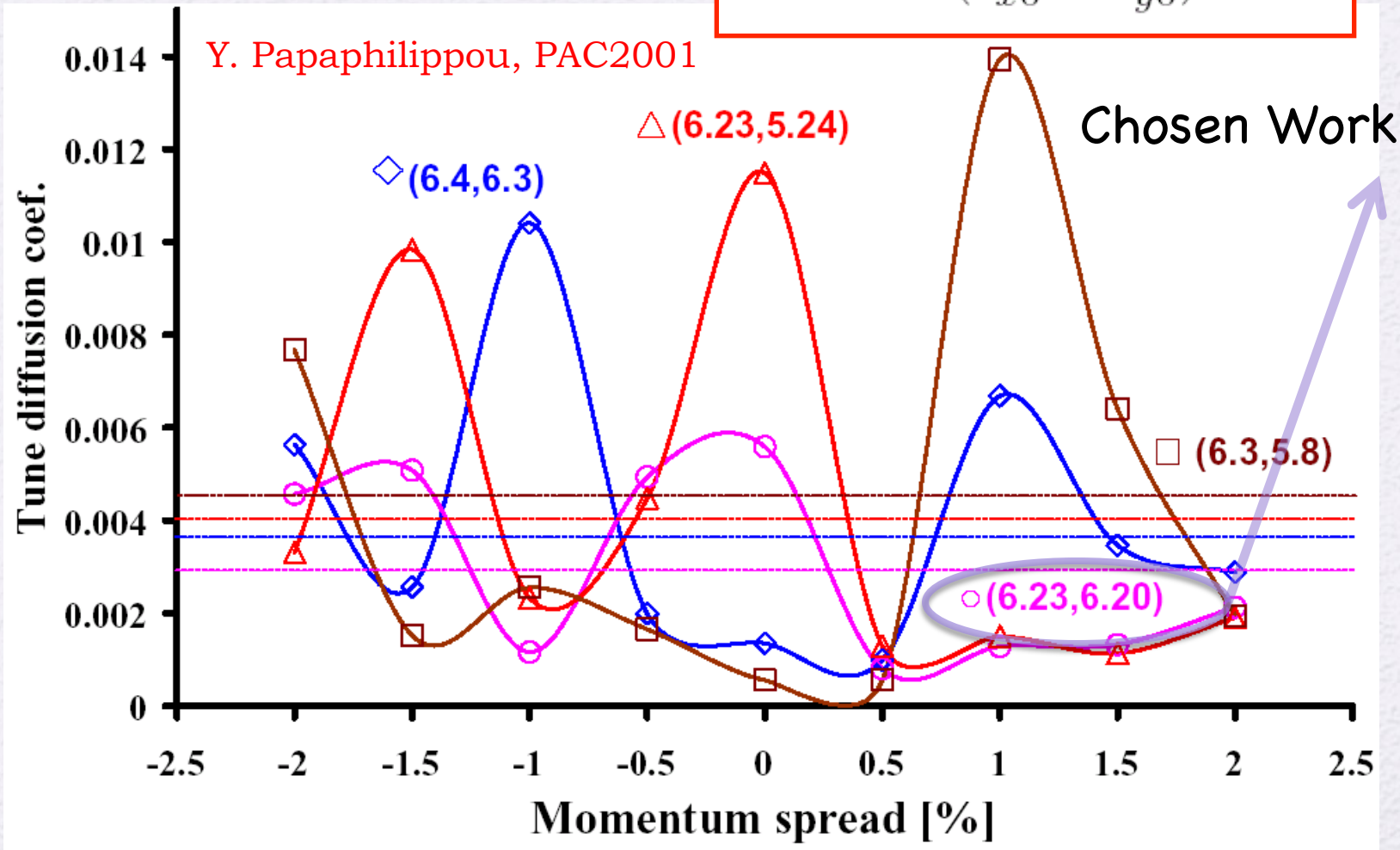

Working point choice for SUPERB

S. Liuzzo et al., IPAC 2012

- The figure of merit for choosing best working point is sum of diffusion rates with a constant added for every lost particle
- Each point is produced after tracking 100 particles
- Nominal working point had to be moved towards "blue" area

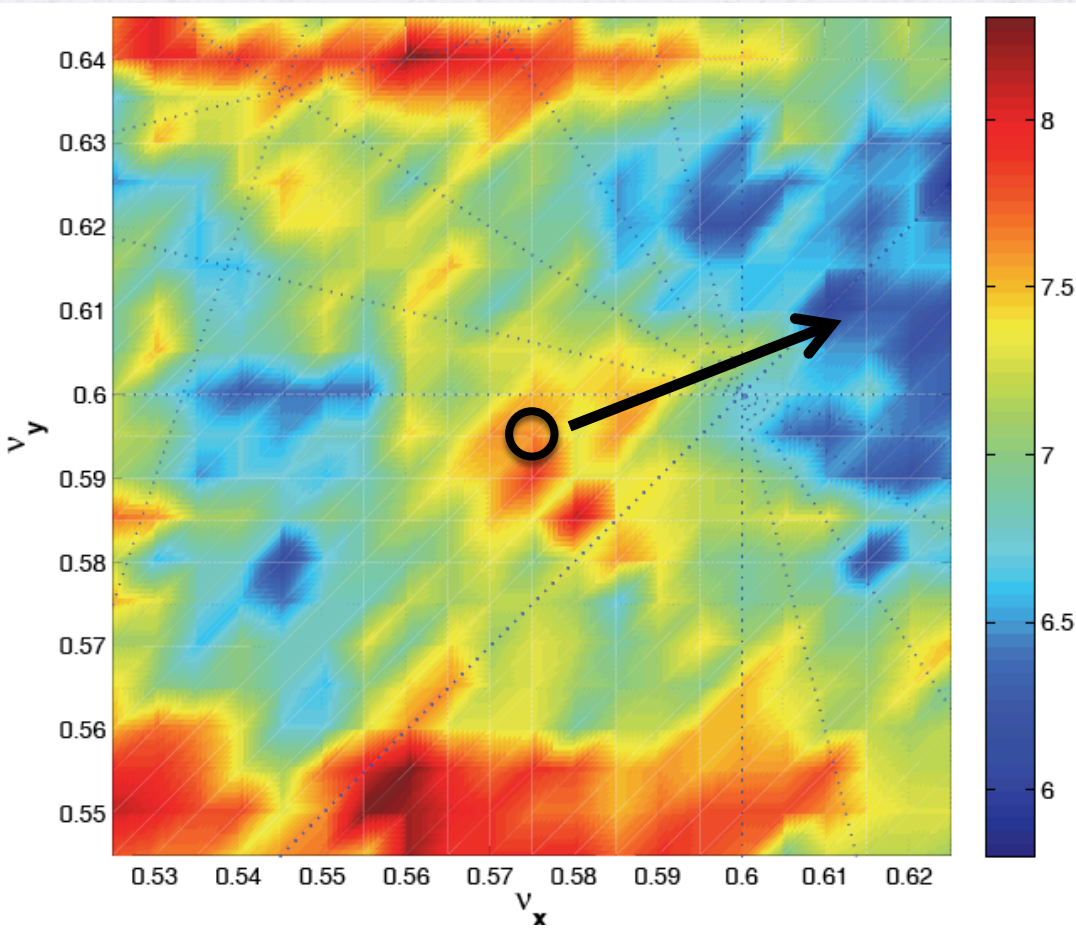

$$e^D = \sqrt{\frac{(\nu_{x,1} - \nu_{x,2})^2 + (\nu_{y,1} - \nu_{y,2})^2}{N/2}}$$

$$WPS = 0.1 N_{lost} + \sum e^D$$

CERN PS2 sextupole scheme optimization

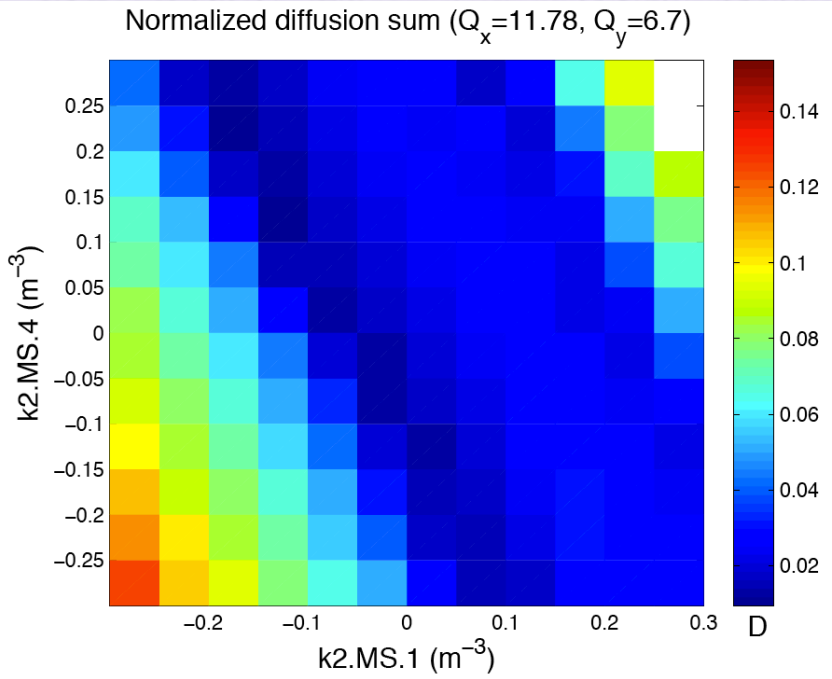

H. Bartosik and Y. P., HB2010, 2010

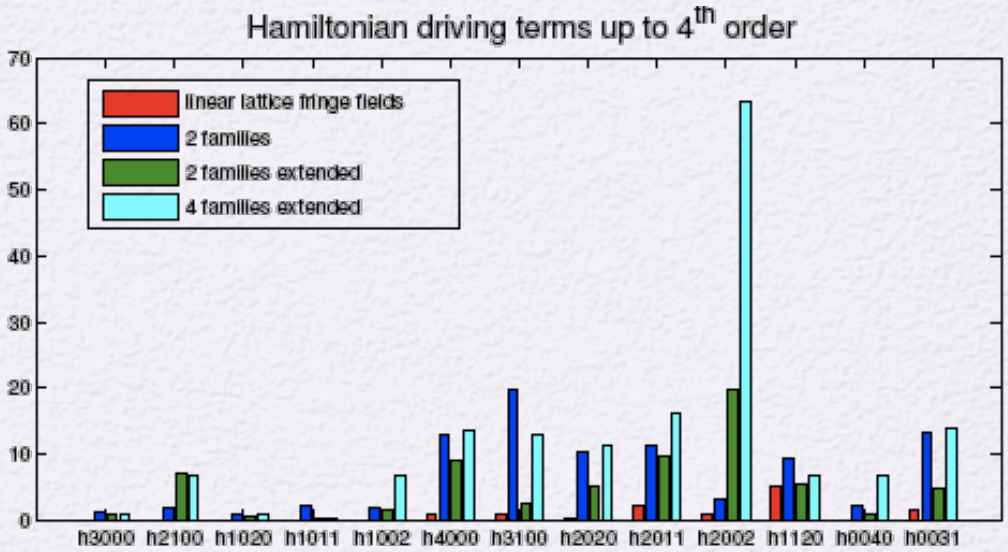

- Comparing different chromaticity sextupole correction schemes and working point optimization using normal form analysis, frequency maps and finally particle tracking
- Finding the adequate sextupole strengths through the tune diffusion coefficient

Experimental frequency maps

D. Robin, et al., PRL 2000

- Frequency analysis of turn-by-turn data of beam oscillations produced by a fast kicker magnet and recorded on a Beam Position Monitors
- Reproduction of the non-linear model of the Advanced Light Source storage ring and working point optimization for increasing beam lifetime

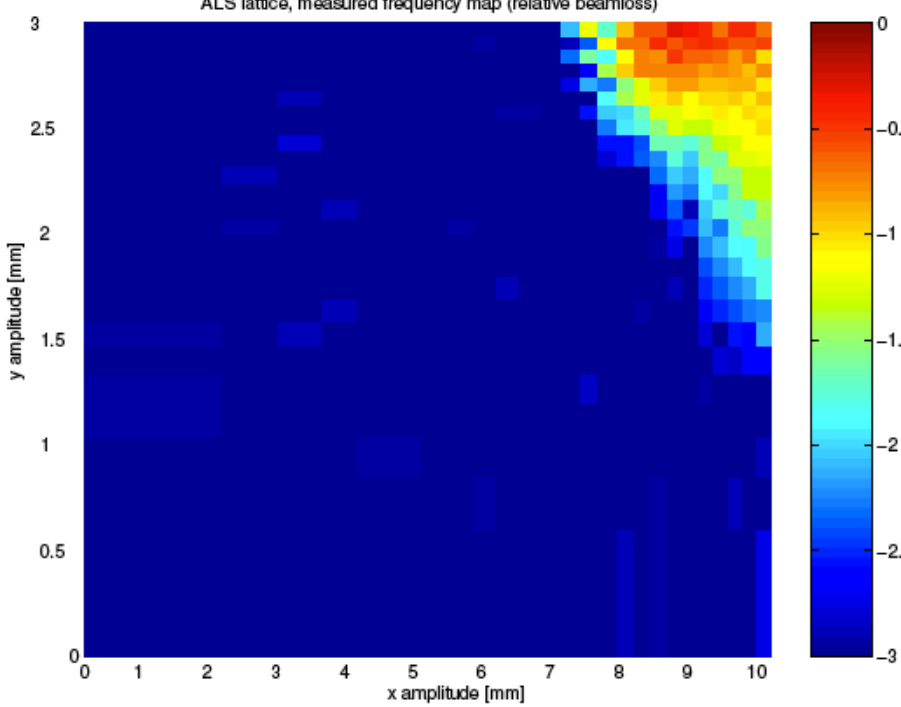

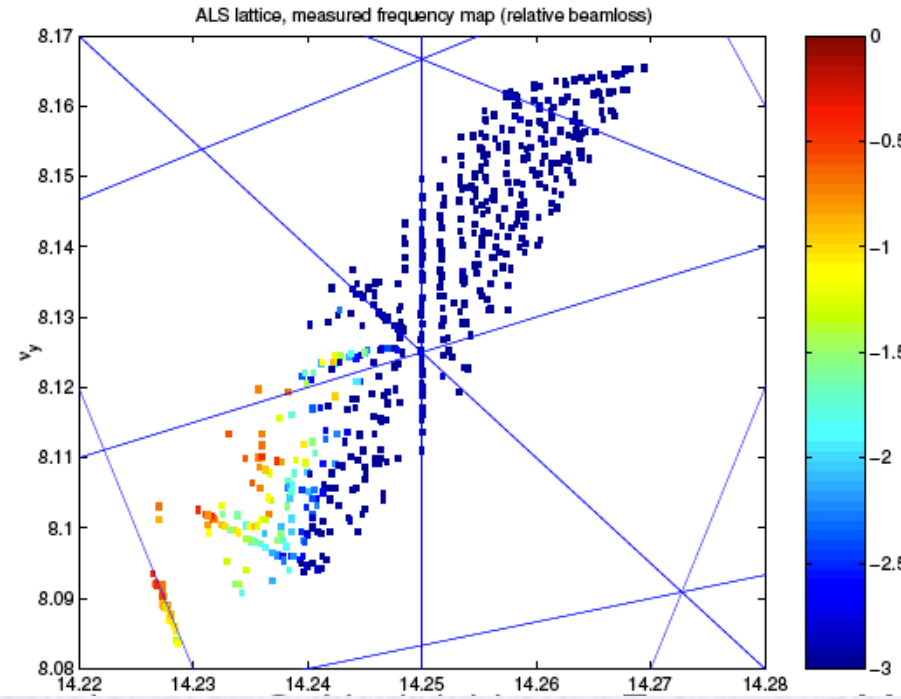

Beam loss frequency maps in the SPS

H. Bartosik, PhD Thesis, Un. Vienna, 2013

- Strength of resonance lines identified by derivative of beam intensity (average beam loss rate)
- Tunes continuously monitored using NAFF and beam intensity recorded with current transformer

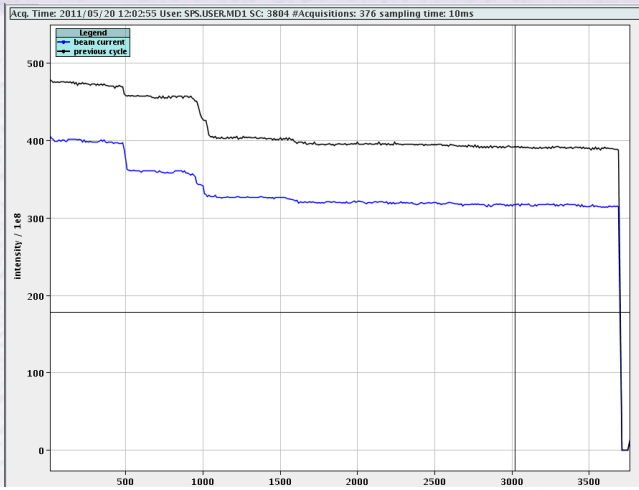

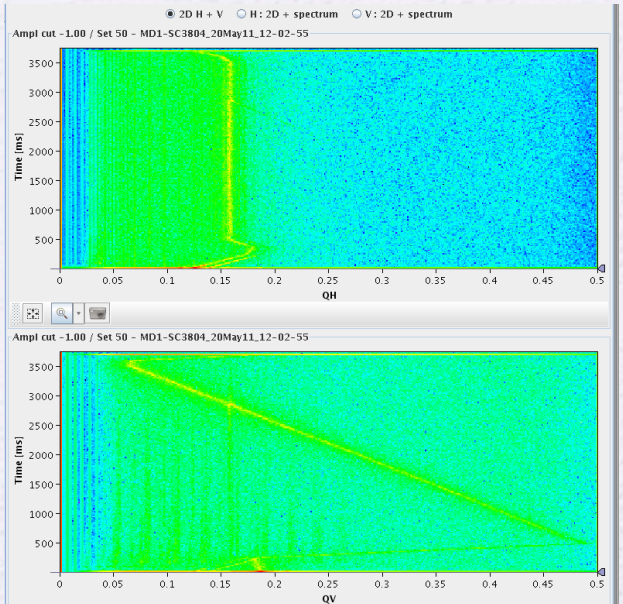

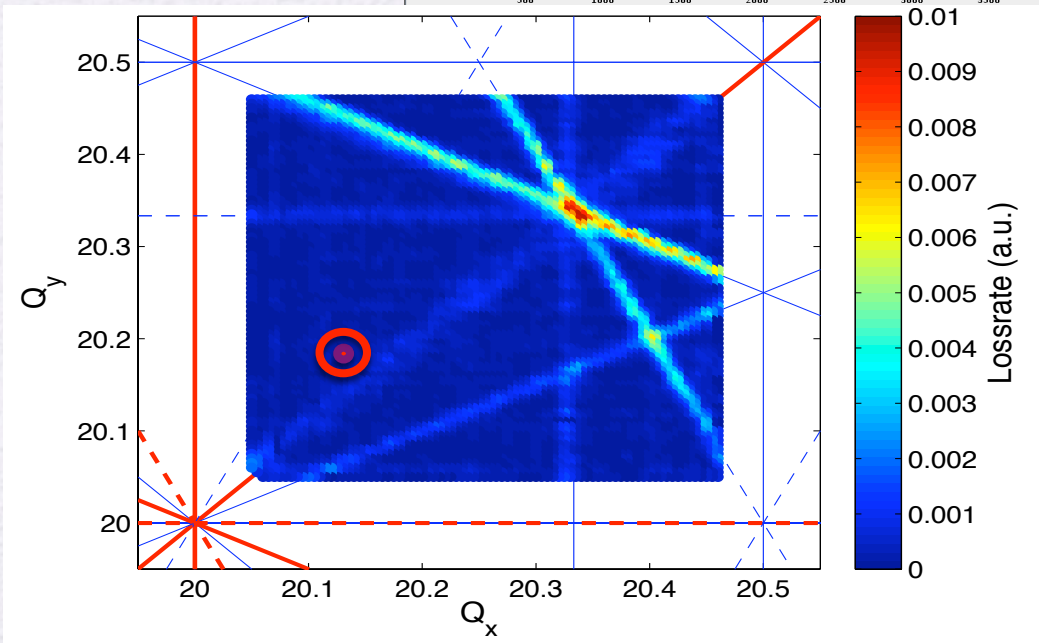

Summary

- Frequency map analysis is a powerful technique for analyzing particle motion in simulations but also in accelerator experiments
- Based on ability to reconstruct numerical quasi-periodic solutions in phase space of general Hamiltonian system
- The power of NAFF algorithm ensures the accurate determination of fundamental frequencies of motions with very high precision precision
- A wide of range of applications for understanding limitations due to non-linear effects in a variety of accelerators
- Application of the method in turn-by-turn data recorded in beam position monitors can reveal effect of non-linear resonances experimentally

Appendix

The NAFF algorithm

- The first frequency ω_1' is found by the location of the maximum of

$$\phi(\sigma) = \langle f(t), e^{i\sigma t} \rangle = \frac{1}{2T} \int_{-T}^{T} f(t) e^{-i\sigma t} \chi(t) dt$$

where $\chi(t)$ is a weight function

- In most of the cases the Hanning window filter is used

$$\chi_1(t) = 1 + \cos(\pi t / T)$$

- Once the first term $e^{i\omega_1' t}$ is found, its complex amplitude a_1' is obtained and the process is restarted on the remaining part of the function

$$f_1(t) = f(t) - a_1' e^{i\omega_1' t}$$

- The procedure is continued for the number of desired terms, or until a required precision is reached

Frequency determination

- The accuracy of an FFT even for a simple sinusoidal signal is not better than

$$|\nu - \nu_T| = \frac{1}{T}$$

- Calculating the Fourier integral explicitly $\phi(\omega) = \frac{1}{T}\int_0^T f(t)e^{-i\omega t}dt$ shows that the maximum lies in between the main picks of the FFT

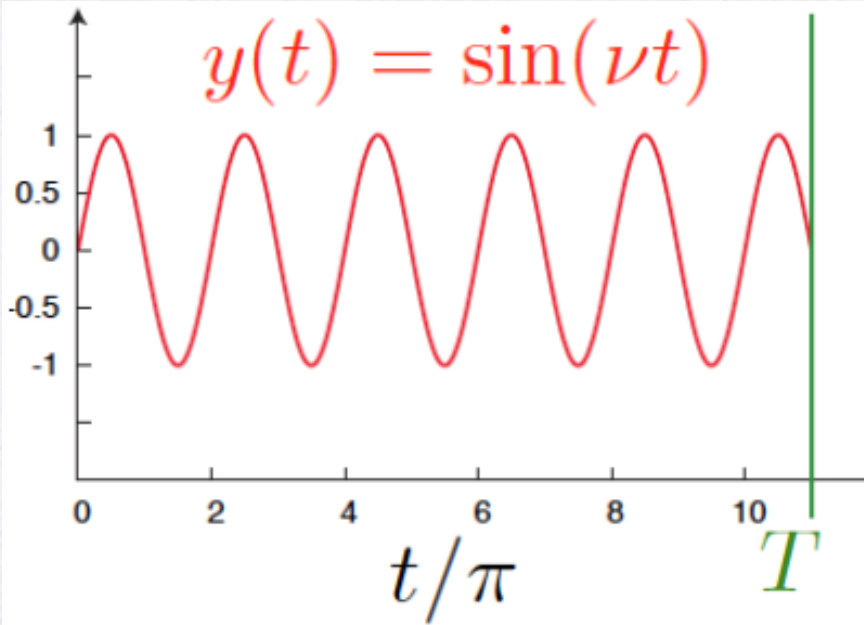

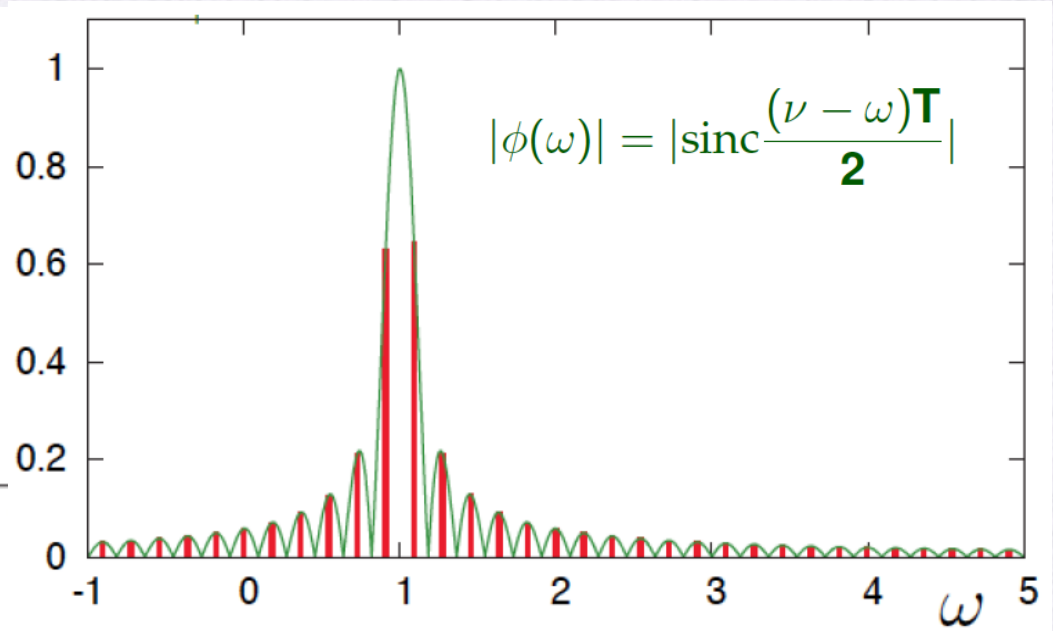

Frequency determination

- A more complicated signal with two frequencies

$$f(t) = a_1 e^{i\omega_1 t} + a_2 e^{i\omega_2 t}$$

shifts slightly the maximum with respect to its real location

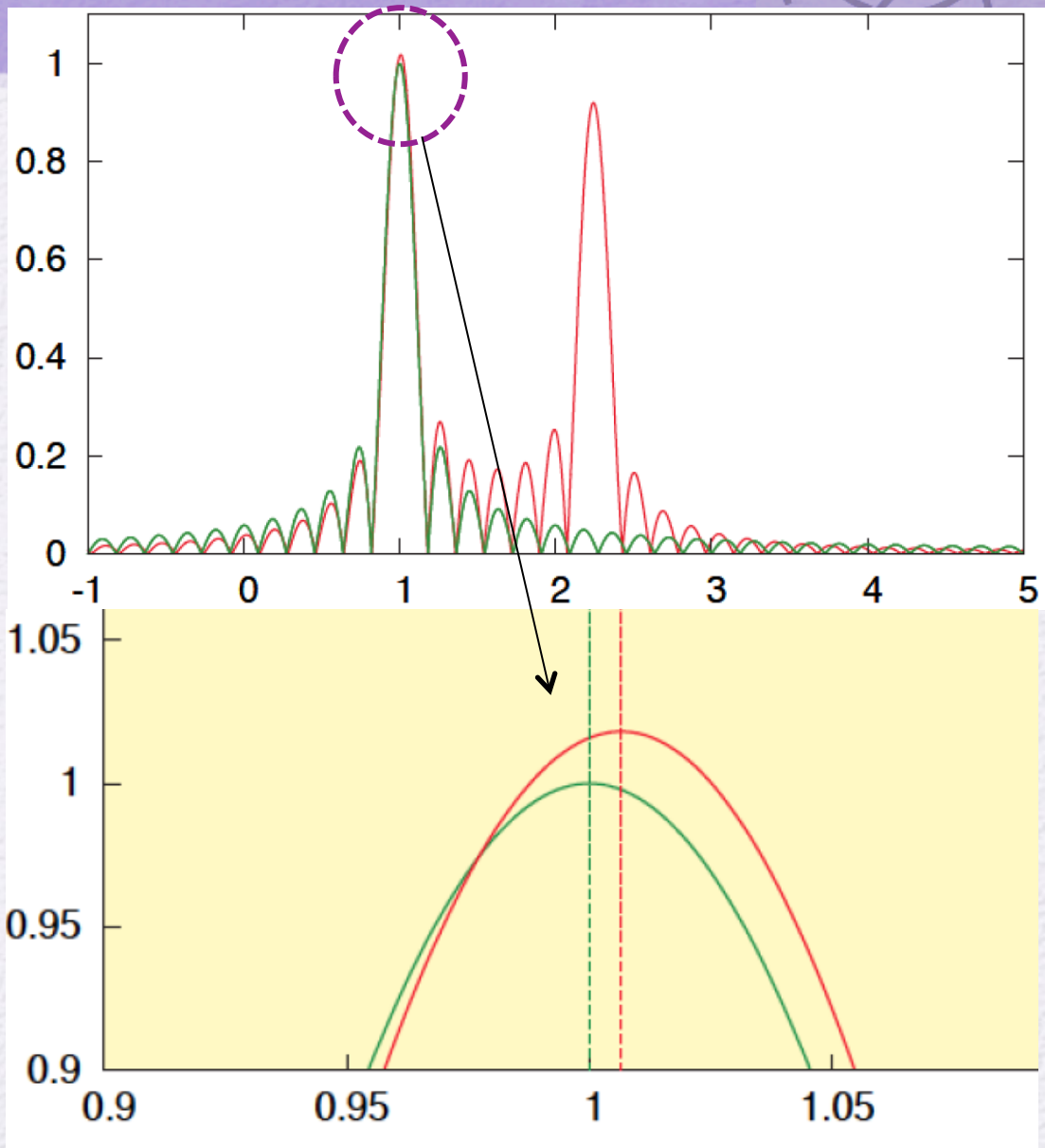

Window function

- A window function like the Hanning filter $\chi_1(t) = 1 + \cos(\pi t/T)$ kills side-lobs and allows a very accurate determination of the frequency

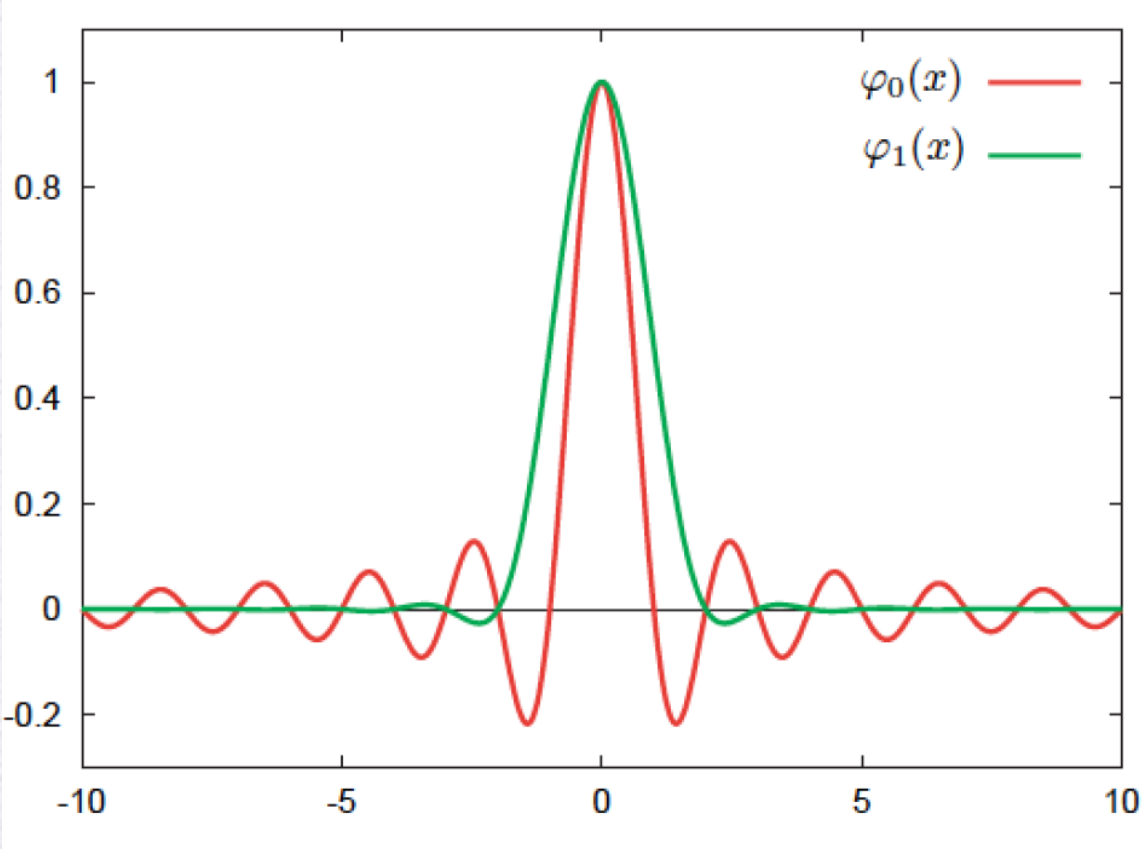

Precision of NAFF

- For a general window function of order p

$$\chi_p(t) = \frac{2^p (p!)^2}{(2p)!}(1+\cos \pi t)^p$$

Laskar (1996) proved a theorem stating that the solution provided by the NAFF algorithm converges asymptotically towards the real KAM quasi-periodic solution with precision

$$\nu_1 - \nu_1^T \propto \frac{1}{T^{2p+2}}$$

- In particular, for no filter (i.e. $p = 0$) the precision is $\frac{1}{T^2}$, whereas for the Hanning filter ($p = 1$), the precision is of the order of $\frac{1}{T^4}$

Folded frequency maps

J.Laskar, PAC2003

- The torsion $M = \left(\frac{\partial \nu(I)}{\partial I}\right) = \left(\frac{\partial^2 H_0(I)}{\partial I^2}\right)$

  with $\nu = \begin{pmatrix}\nu_1 \\ \nu_2\end{pmatrix} = M \begin{pmatrix} I_1 \\ I_2 \end{pmatrix}$

- Hamiltonian $H = \frac{1}{2} I^\tau M I + o(I^2) + O(\varepsilon)$
- For a fixed energy value and even in the presence of chaos $I^\tau M I \approx 2h = Cte$

  or $\nu^\tau M^{-1} \nu \approx 2h = Cte$
- For an accelerator $M^{-1} = \begin{pmatrix} a & c \\ c & b \end{pmatrix}$ is symmetric

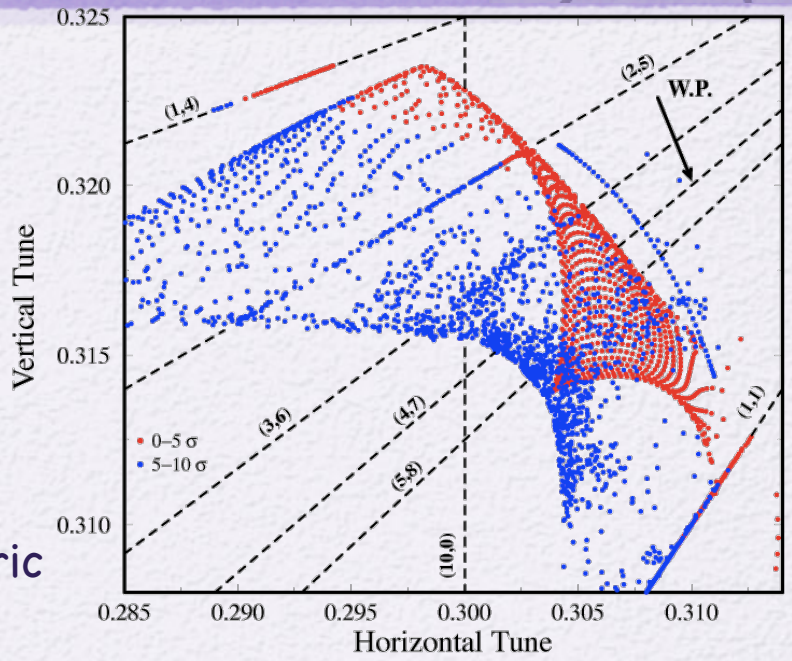

$\det(M) > 0$

no isotropic directions

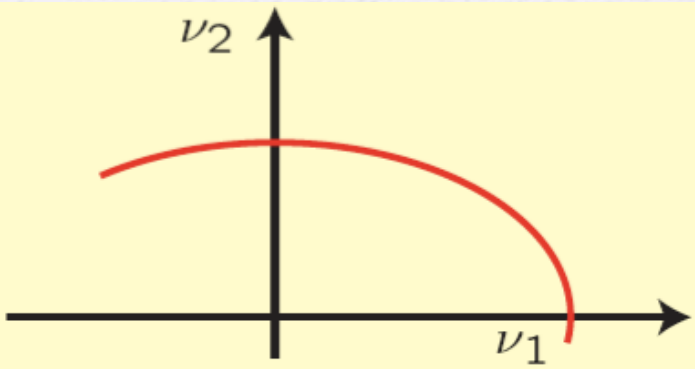

$\det(M) < 0$

isotropic direction

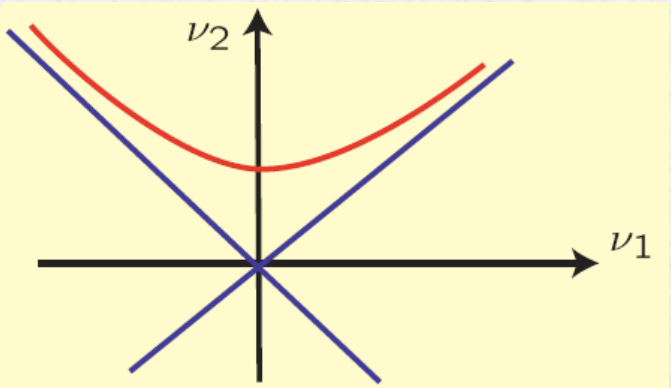

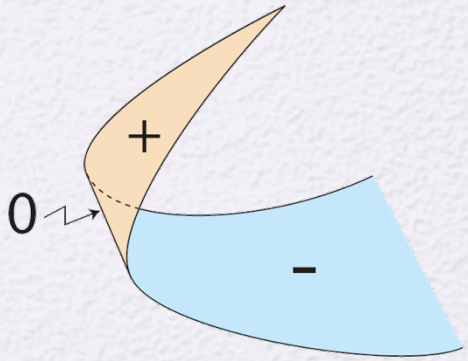

Application of the $SABA_2C$ integrator to accelerators

Ch. Skokos, et al., EPAC 2008

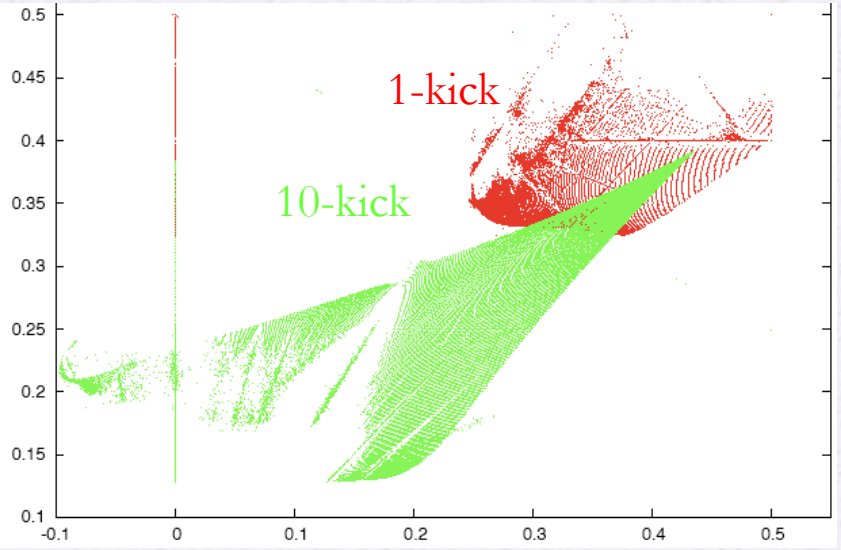

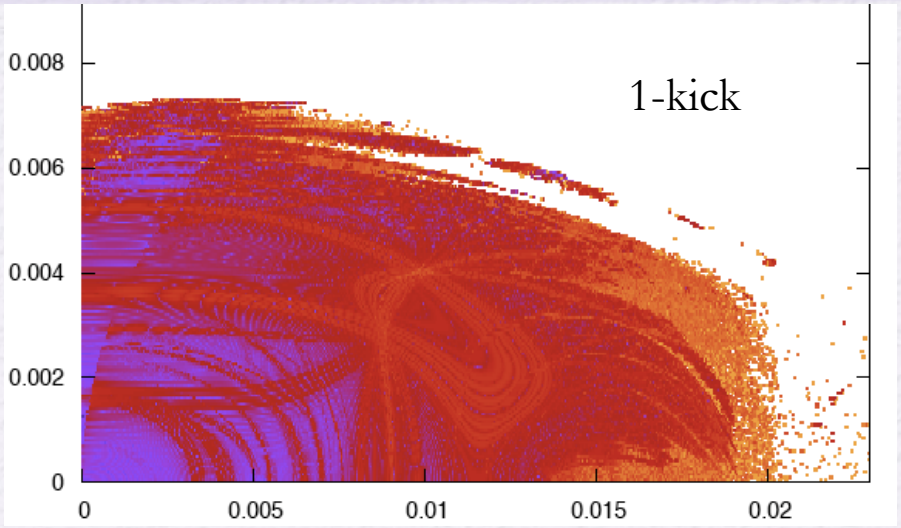

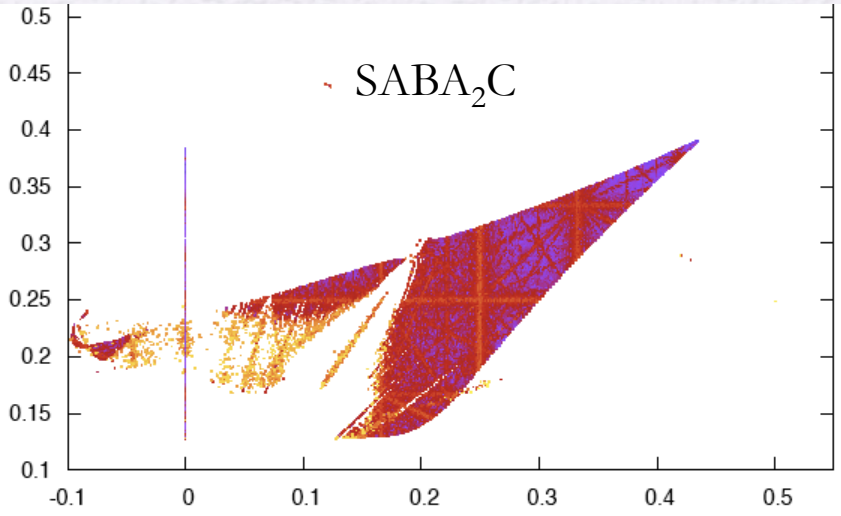

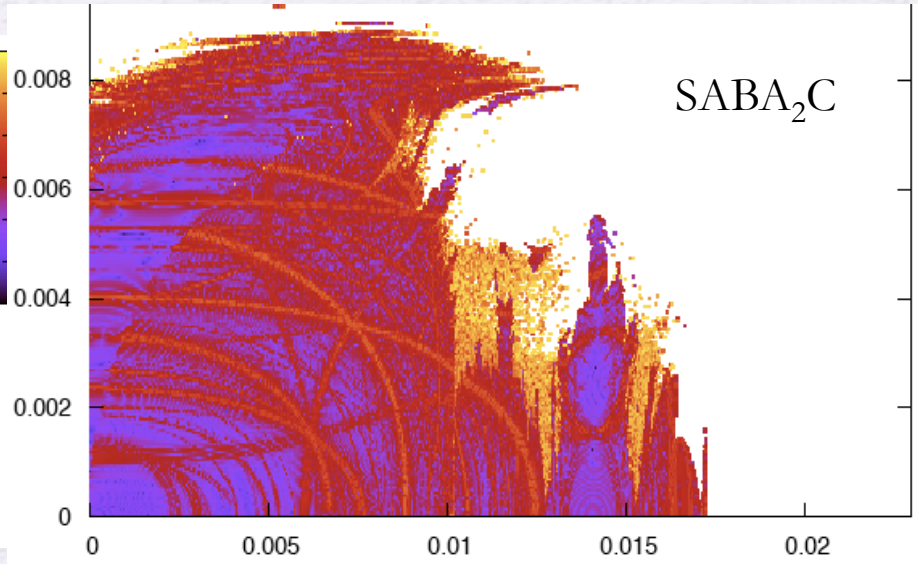

CLIC Pre-damping rings

F. Antoniou, PhD thesis, NTUA, 2013

- Non linear optimization based on phase advance scan for minimization of resonance driving terms and tune-shift with amplitude

$$\left|\sum_{p=0}^{N_c-1} e^{ip(n_x\mu_{x,c}+n_y\mu_{y,c})}\right| = \sqrt{\frac{1-\cos\left[N_c(n_x\mu_{x,c}+n_y\mu_{y,c})\right]}{1-\cos(n_x\mu_{x,c}+n_y\mu_{y,c})}} = 0$$

$$N_c(n_x\mu_{x,c}+n_y\mu_{y,c}) = 2k\pi$$

$$n_x\mu_{x,c}+n_y\mu_{y,c} \neq 2k'\pi$$

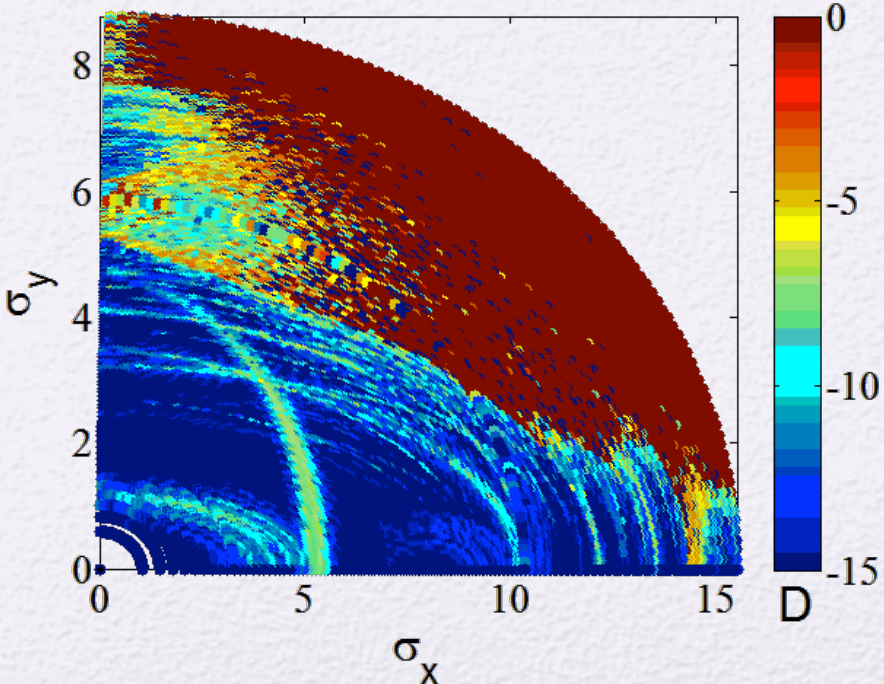

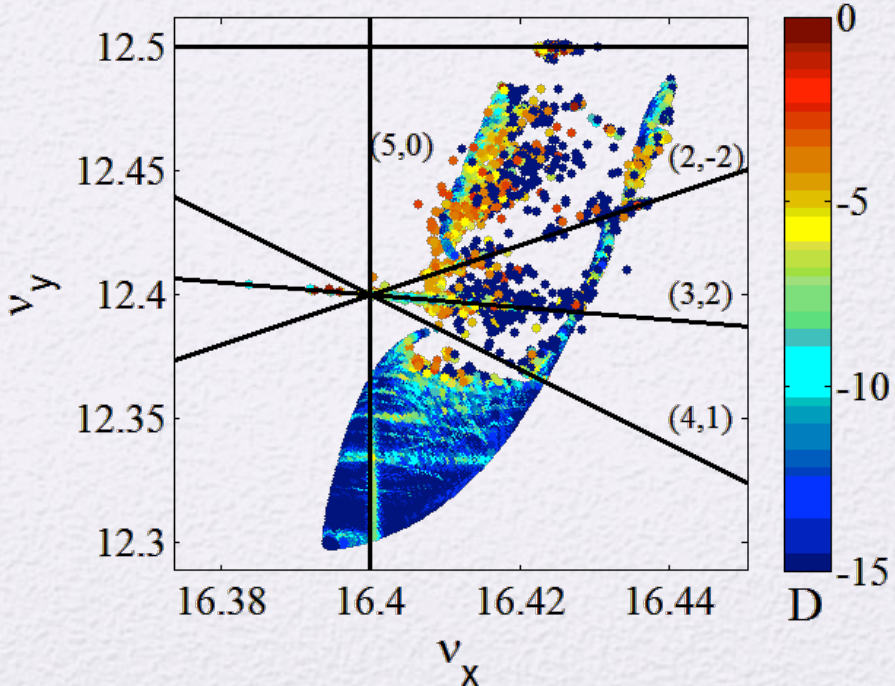

Experimental non-linear dynamics at the ESRF

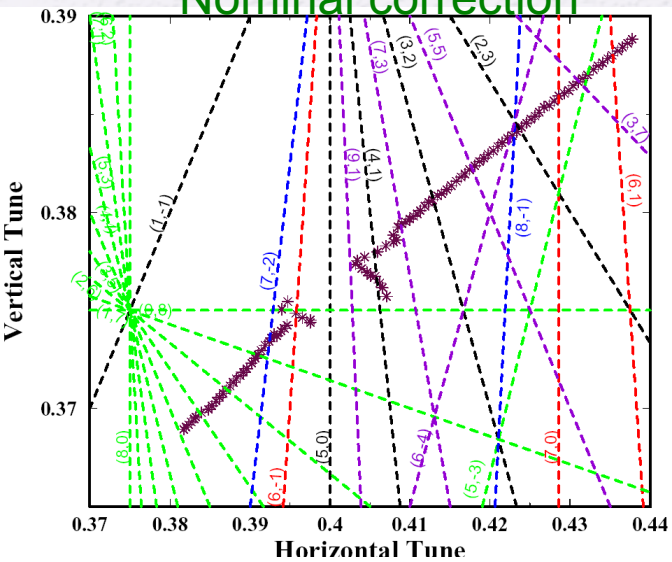

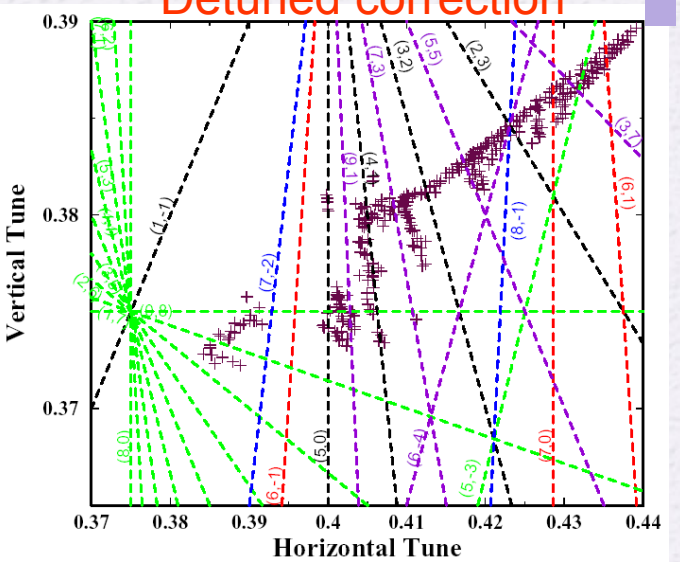

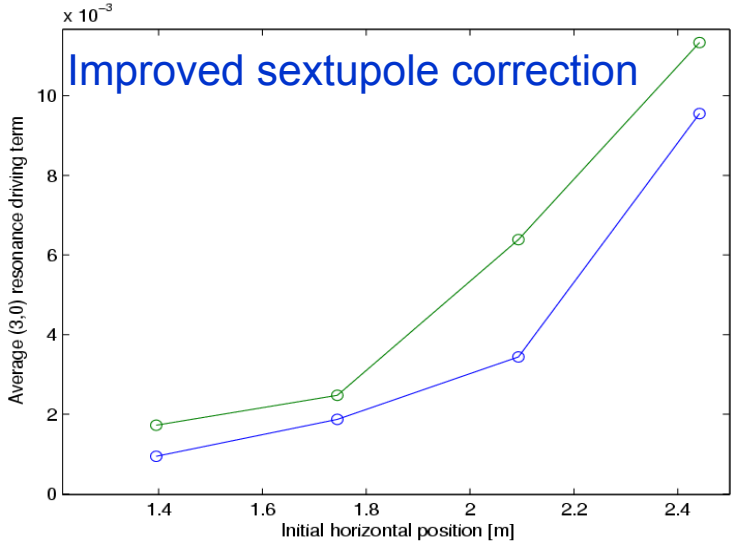

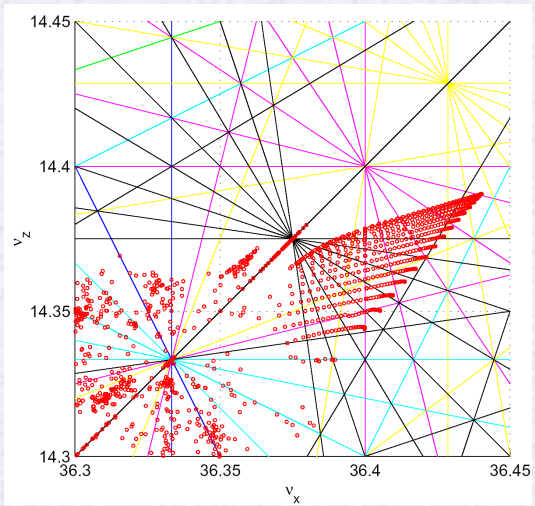

- 3 regions:
  - Small amplitudes: regular motion
  - Medium amplitudes: 5th order resonance crossing
  - Large amplitudes: losses due to 3rd order resonance crossing
- Excitation of 3rd order resonance and correction with sextupole correctors
- Refinement of the non-linear model

Y. P. et al. EPAC 2004

Space charge frequency scan

H. Bartosik, PhD Thesis, Un. Vienna, 2013

- Injecting high bunch density beam into the SPS
- Space charge effect quite strong with (linear) tune-shifts of $\Delta Q_x/\Delta Q_y \sim 0.10/0.18$
- Changing horizontal/vertical frequency and measuring emittance (action) blow-up

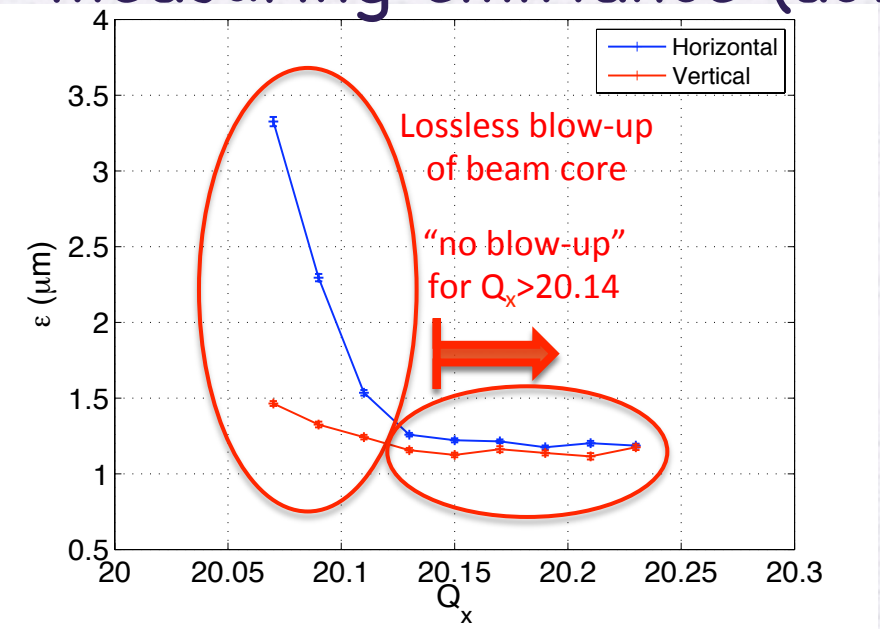

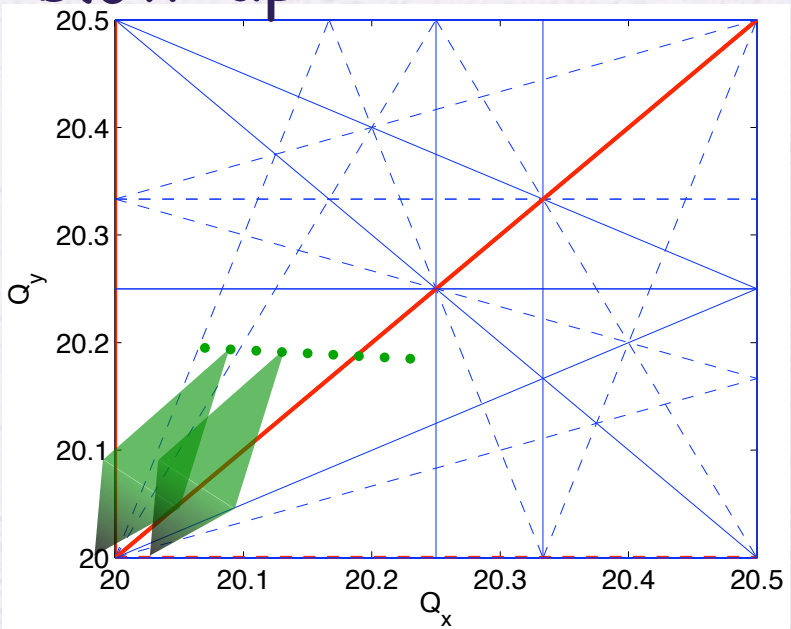

Space charge frequency scan

H. Bartosik, PhD Thesis, Un. Vienna, 2013

- Injecting high bunch density beam into the SPS
- Space charge effect quite strong with (linear) tune-shifts of $\Delta Q_x/\Delta Q_y \sim 0.10/0.18$
- Changing horizontal/vertical frequency and measuring emittance (action) blow-up